

LA-UR-17-21218

Approved for public release; distribution is unlimited.

Title: (U) An Analytic Study of Piezoelectric Ejecta Mass Measurements

Author(s): Tregillis, Ian Lee

Intended for: Report

Issued: 2017-02-16

Disclaimer:

Los Alamos National Laboratory, an affirmative action/equal opportunity employer, is operated by the Los Alamos National Security, LLC for the National Nuclear Security Administration of the U.S. Department of Energy under contract DE-AC52-06NA25396. By approving this article, the publisher recognizes that the U.S. Government retains nonexclusive, royalty-free license to publish or reproduce the published form of this contribution, or to allow others to do so, for U.S. Government purposes. Los Alamos National Laboratory requests that the publisher identify this article as work performed under the auspices of the U.S. Department of Energy. Los Alamos National Laboratory strongly supports academic freedom and a researcher's right to publish; as an institution, however, the Laboratory does not endorse the viewpoint of a publication or guarantee its technical correctness.

(U) An Analytic Study of Piezoelectric Ejecta Mass Measurements

I. L. Tregillis
Plasma Theory and Applications, XCP-6
Los Alamos National Laboratory
Los Alamos, NM 87545

Abstract

We consider the piezoelectric measurement of the areal mass of an ejecta cloud, for the specific case where ejecta are created by a single shock at the free surface and fly ballistically through vacuum to the sensor. To do so, we define time- and velocity-dependent ejecta “areal mass functions” at the source and sensor in terms of typically unknown distribution functions for the ejecta particles. Next, we derive an equation governing the relationship between the areal mass function at the source (which resides in the rest frame of the free surface) and at the sensor (which resides in the laboratory frame). We also derive expressions for the analytic (“true”) accumulated ejecta mass at the sensor and the measured (“inferred”) value obtained via the standard method for analyzing piezoelectric voltage traces. This approach enables us to derive an exact expression for the error imposed upon a piezoelectric ejecta mass measurement (in a perfect system) by the assumption of instantaneous creation. We verify that when the ejecta are created instantaneously (i.e., when the time dependence is a delta function), the piezoelectric inference method exactly reproduces the correct result. When creation is not instantaneous, the standard piezo analysis will always overestimate the true mass. However, the error is generally quite small (less than several percent) for most reasonable velocity and time dependences. In some cases, errors exceeding 10-15% may require velocity distributions or ejecta production timescales inconsistent with experimental observations. These results are demonstrated rigorously with numerous analytic test problems.

Contents

1	Introduction	1
2	Definitions and derivations	2
2.1	Kinematics	2
2.2	Distribution functions and areal mass functions	4
2.3	Relationship between m_a and m_c	5
2.4	Pressure and accumulated areal mass	6
2.5	Time-dependent u_{fs}	7
3	General expression for the error in the inferred areal mass, χ	9
3.1	Instantaneous creation	14
3.2	Stationary velocity distributions	14
3.3	Time-dependent u_{fs}	15
4	Analytic test problems with stationary velocity distributions	16
4.1	Delta function properties	16
4.2	TP 1: Instantaneous production, single fixed velocity	17
4.3	TP 2: Sustained production, single fixed velocity	20
4.4	TP 3: Instantaneous production, power law velocity distribution	25
4.5	TP 4: RMI source model, single fixed velocity	28
4.6	General case: Instantaneous production	32
4.7	General case: Sustained constant production	34
4.8	General case: Arbitrary time dependence, single fixed velocity	37
4.9	General case: Arbitrary time dependence, arbitrary stationary velocity distribution	42
5	Analytic test problems with nonstationary velocity distributions	46
5.1	TP5: RMI source model, single linearly increasing velocity	46
5.2	General case: Arbitrary time dependence, single linearly increasing velocity	61
5.3	General case: Arbitrary time dependence, single arbitrary velocity	66
A	Inference of Dynamical Quantities and Ejecta Areal Mass from Piezoelectric Voltages	69
References		72

1 Introduction

This document contains mathematical notes pertaining to the problem of measuring the areal mass of an ejecta cloud through the use of a piezoelectric sensor. The present analysis applies strictly to the situation where ejecta production is the result of a single shock, and where all transport between the source and sensor occurs in vacuum. This analysis does not apply to double-shock experiments, nor to cases where the ejecta are transported through a gaseous medium. The current treatment assumes negligible deceleration of the free surface during an extended ejecta creation interval, although the situation may differ in the case of an unsupported shock.

We begin in Section 2 by defining the problem geometry and establishing several fundamental relationships. Then we derive the fundamental equation governing coordinate transformations between the source (i.e., free-surface) and sensor (i.e., laboratory) rest frames. This enables us to derive expressions for both the analytic (“true”) and measured (“inferred”) accumulated ejecta mass at the sensor, for a given analytic function describing the time- and velocity-dependent areal mass at the source. In Section 3, we use these results to derive a general expression for the error, χ . This leads to a simple upper bound on the error percentage imposed (on a perfect system) by the assumption of instantaneous ejecta creation. This bound arises strictly from kinematic considerations; it does not rely upon assumptions about the velocity or size distributions of the ejecta particles.

Following the general result, we demonstrate specific cases by applying these derivations to a series of analytic test problems. In particular, Section 4 focuses on stationary velocity distributions, while Section 5 examines the more complex case of non-stationary (time-dependent) velocity distributions. Appendix A summarizes the procedure for extracting a time-dependent ejecta areal mass from piezoelectric voltage traces.

This document is meant to function as a complete transcription of handwritten explorations of this problem, rather than a journal paper draft. Intermediate mathematical steps are retained here as an aid to verifying the derivations and conclusions. A paper draft derived from this document will be considerably shorter.

2 Definitions and derivations

We begin by introducing all definitions, conventions, and derivations used throughout this analysis.

2.1 Kinematics

All definitions are derived from the problem geometry depicted in Figure 1.

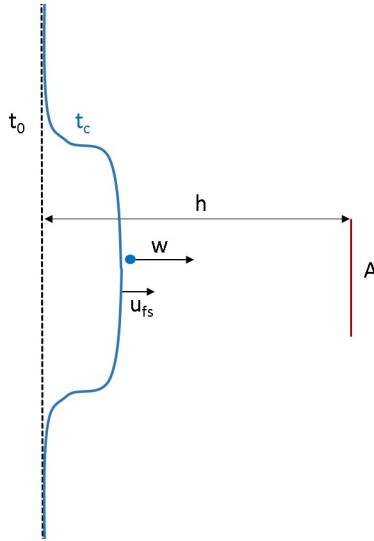


Figure 1: Cartoon depiction of the problem geometry. The dashed line (black) represents the initial (unperturbed) free surface at the shock breakout time, t_0 . The solid line (blue) represents the free surface at the creation time (t_c) for a given particle of interest, which is born with velocity w relative to the free surface. The free surface is assumed to undergo instantaneous acceleration to constant velocity u_{fs} at the instant of shock breakout. The known initial distance from the unperturbed free surface to the piezoelectric sensor (with collecting area A) is h . (All calculations in this treatment assume a uniformly accelerated free surface.)

Let us define the shock breakout time (t_0), the time of ejecta particle creation (t_c), and the time of particle arrival at the sensor (t). Our convention is that velocities measured relative to the free surface are denoted w , and that velocities measured relative to the motionless sensor (i.e., in the lab frame) are denoted u . The free surface velocity in the lab frame is u_{fs} (assumed constant in this treatment). A

particle with velocity w relative to the free surface has velocity $u = w + u_{fs}$ relative to the sensor. We define all times and velocities to be positive, and only consider times prior to the arrival of the free surface at the sensor.

For a particle created (i.e., ejected from the free surface) at time t_c with relative velocity w , the arrival time at the sensor, t , will be given by

$$t(w, t_c) = t_c + \frac{h - u_{fs}(t_c - t_0)}{w + u_{fs}} = \frac{wt_c + (h + u_{fs}t_0)}{w + u_{fs}}. \quad (2.1)$$

This is simply the creation time plus the transit time from the free surface location at time t_c to the static pin location; $u_{fs}(t_c - t_0)$ is the distance traveled by the free surface between the shock breakout and particle creation times. (Notice that when $t_c = t_0$ (i.e., when the ejecta particle is created at the instant of shock breakout) the arrival time is the creation time plus the time of flight; when $t_c = t_0 = 0$, the arrival time is simply the time of flight.) From this we can obtain the creation time, t_c , required for a particle with relative velocity w to arrive at the sensor at time t :

$$t_c(w, t) = \frac{(w + u_{fs})t - (h + u_{fs}t_0)}{w}. \quad (2.2)$$

Both $t(w, t_c)$ and $t_c(w, t)$ can be converted to functions of lab-frame velocity, u , via the substitution $w = u - u_{fs}$. The lab-frame velocity required such that a particle created at time t_c arrives at the sensor at a specified time t is straightforward:

$$u(t_c, t) = \frac{h - u_{fs}(t_c - t_0)}{t - t_c} \quad (2.3)$$

from which we obtain the associated relative velocity:

$$w(t_c, t) \equiv u(t_c, t) - u_{fs} = \frac{h - u_{fs}(t_c - t_0)}{t - t_c} - u_{fs} = \frac{h - u_{fs}(t - t_0)}{t - t_c}. \quad (2.4)$$

Note that Equations 2.1 and 2.2 imply that for a *fixed* velocity, w ,

$$\frac{dt}{dt_c} = \left(\frac{w}{w + u_{fs}} \right) = \left(\frac{u - u_{fs}}{u} \right) \quad (2.5)$$

$$\frac{dt_c}{dt} = \left(\frac{w + u_{fs}}{w} \right) = \left(\frac{u}{u - u_{fs}} \right). \quad (2.6)$$

Consider particles of a fixed relative velocity w , emitted continuously during a creation interval Δt_c . Their arrival interval at the sensor, Δt , will be shorter than Δt_c because the free surface approaches the sensor during the emission interval, meaning particles emitted later in the interval travel a shorter distance at the same velocity than particles emitted earlier in the interval. Thus $\Delta t_c > \Delta t$ for a fixed velocity.

2.2 Distribution functions and areal mass functions

Microphysics at the free surface determines, either explicitly or implicitly, a distribution function for the ejecta particles. In particular, we define

$$f_c(m, w, t_c) dm dw dt_c \quad (2.7)$$

to be the number of ejecta particles created at time t_c with mass in the range $[m, m + dm]$ and relative velocity in the range $[w, w + dw]$. Then it follows

$$\iiint f_c(m, w, t_c) dm dw dt_c = N_t \quad (2.8)$$

where N_t is the total number of ejecta particles created at the free surface, and thus

$$f_c = \frac{dN(m, w, t_c)}{dm dw dt_c} \quad (2.9)$$

where $N(m, w, t_c)$ is the number of ejecta particles created at time t_c with mass m and relative velocity w . The units of f_c must be $[\text{mass}^{-1} \cdot \text{velocity}^{-1} \cdot \text{time}^{-1}]$ or $[\text{mass}^{-1} \cdot \text{length}^{-1}]$.

The total ejecta mass is given by

$$\iiint m f_c(m, w, t_c) dm dw dt_c = M_t \quad (2.10)$$

so

$$\int m f_c(m, w, t_c) dm = \frac{dM}{dw dt_c} \quad (2.11)$$

where $M(w, t_c)$ is the ejecta mass created at time t_c with relative velocity w .

We can now define the *areal mass function* for particles of relative velocity w created at the time t_c :

$$m_c(w, t_c) \equiv \frac{1}{A} \int m f_c(m, w, t_c) dm. \quad (2.12)$$

The units of m_c are $[\text{mass} \cdot \text{area}^{-1} \cdot \text{velocity}^{-1} \cdot \text{time}^{-1}]$ or $[\text{mass} \cdot \text{volume}^{-1}]$.

Similar reasoning may be applied to the distribution function, f_a , of particles arriving at the piezoelectric sensor in the lab frame. In that fashion we obtain the areal mass function for particles of lab-frame velocity u arriving (collected) at time t :

$$m_a(u, t) \equiv \frac{1}{A} \int m f_a(m, u, t) dm. \quad (2.13)$$

The lab-frame areal mass function m_a has the same units as m_c .

Because m_c is determined by microphysics of ejecta production at the free surface, it is defined in the rest frame of the free surface. Alternatively, because m_a is determined by the distribution of ejecta particles arriving at the sensor, it is most sensible to define that function in the lab frame.

Note furthermore that specific knowledge of the distribution functions f_c and f_a is unnecessary for our purposes. It is sufficient to know the areal mass functions can be related to the microphysics of ejecta production via the (possibly unknown) distribution functions.

2.3 Relationship between m_a and m_c

Our goal is to investigate how reliably quantities inferred from sensor measurements reflect the true (analytic) situation. To do that, we must first derive a relationship between m_a and m_c .

We assume all ejecta particles created at the free surface eventually arrive at the sensor, and that the motion is collinear so that the relevant area does not change. (See Appendix A for a full description of the assumptions underlying the piezoelectric sensor analysis.) Thus a particle arriving at the detector at time t with lab-frame velocity u must have been created at the free surface with relative velocity $w = u - u_{fs}$ at time t_c ($u - u_{fs}, t$). We therefore expect

$$m_a(u, t) \propto m_c[u - u_{fs}, t_c(u - u_{fs}, t)].$$

Mass conservation implies

$$m_a(u, t) du dt = m_c(w, t_c) dw dt_c$$

or

$$m_a(u, t) = \frac{dw}{du} \frac{dt_c}{dt} m_c(w, t_c) = \left(\frac{w + u_{fs}}{u} \right) m_c(w, t_c),$$

from which we obtain the fundamental equation relating the source (m_c) and sensor (m_a) areal mass functions:

$$m_a(u, t) = \left(\frac{u}{u - u_{fs}} \right) m_c \left[u - u_{fs}, \frac{ut - (h + u_{fs}t_0)}{u - u_{fs}} \right].$$

(2.14)

Equation 2.14 can be confirmed by computing the total ejecta mass created at the free surface and collected at the sensor. Conservation of mass requires

$$A \int_0^\infty \int_0^\infty m_c(w, t_c) dw dt_c = A \int_0^\infty \int_0^\infty m_a(u, t) du dt.$$

Applying Equation 2.14 and the substitutions

$$x = u - u_{fs} \quad y = \frac{ut - (h + u_{fs}t_0)}{u - u_{fs}}$$

to the right-hand expression (the total mass collected at the sensor) yields

$$\begin{aligned} & A \int_0^\infty \int_0^\infty \left(\frac{u}{u - u_{fs}} \right) m_c \left[u - u_{fs}, \frac{ut - (h + u_{fs}t_0)}{u - u_{fs}} \right] du dt \\ &= A \int_{-u_{fs}}^\infty \int_{-\frac{h+u_{fs}t_0}{u-u_{fs}}}^\infty \left(\frac{x + u_{fs}}{x} \right) m_c(x, y) \left(\frac{x}{x + u_{fs}} \right) dx dy. \end{aligned}$$

Because the problem is defined such that all velocities and times are positive, $m_c(x, y) = 0$ for both $x < 0$ and $y < 0$. Thus the right-hand expression becomes

$$A \int_0^\infty \int_0^\infty m_c(x, y) dx dy$$

which is exactly equivalent to the left-hand expression (the total mass ejected by the free surface). This demonstrates that mass is conserved.

Thus, Equation 2.14 is the correct relationship between the areal mass functions at the source and sensor.

2.4 Pressure and accumulated areal mass

We can now write expressions for the time-dependent pressures on the free surface and the sensor, and for the time-dependent accumulated areal mass at the sensor, given an areal mass function at the source.

The pressure on the free surface is equivalent to the recoil momentum flux. This is simply

$$P_c(t_c) = \int_0^\infty m_c(w, t_c) w dw. \quad (2.15)$$

Similarly, the pressure on the sensor is given by

$$P(t) = \int_0^\infty m_a(u, t) u \, du = \int_0^\infty \left(\frac{u^2}{u - u_{fs}} \right) m_c \left[u - u_{fs}, \frac{ut - (h + u_{fs}t_0)}{u - u_{fs}} \right] \, du \quad (2.16)$$

The *analytic* (“true”) mass per unit area accumulated at the sensor is clearly

$$m_t(t) = \int_0^t dt' \int_0^\infty m_a(u, t') \, du \quad (2.17)$$

(note this becomes the total accumulated mass as $t \rightarrow \infty$). We choose this form for simplicity, although clearly $m_t(t) = 0$ for $0 < t < t_0^a$ where t_0^a is the earliest particle arrival time at the sensor; likewise, of course, $m_a(u, t) = 0$ for $u \leq u_{fs}$.

Meanwhile, and as shown in Appendix A, the accumulated ejecta mass per unit area *inferred* from the piezoelectric sensor measurement is

$$m_i(t) = \int_0^t \left(\frac{t' - t_0}{h} \right) P(t') \, dt' = \frac{1}{h} \int_0^t dt' \int_0^\infty m_a(u, t') u (t' - t_0) \, du \quad (2.18)$$

where $P(t)$ is the pressure measured by the sensor, i.e., Equation 2.16. The preceding observation regarding the integration limits applies here, as well: we choose this form for simplicity, although both lower limits of integration could be increased to positive values without changing the evaluation.

Equations 2.15 - 2.18 embody everything we need to examine the piezoelectric mass measurement procedure analytically.

We can also compute an analytic expression for the time-dependent voltage at the pin. As explained in Appendix A, the voltage is given by

$$V(t) = A R S \frac{dP}{dt} \quad (2.19)$$

where $P(t)$ is again given by Equation 2.16, R is the terminating resistance of the circuit, and S is the piezoelectric sensitivity.

2.5 Time-dependent u_{fs}

Throughout, this treatment assumes the free-surface velocity to be constant. Here we comment briefly on the situation $u'_{fs}(t_c) \neq 0$.

In this case, the distance traveled by the free surface between times t_0 and t_c is

$$\Delta h = \int_{t_0}^{t_c} u_{fs}(t'_c) dt'_c,$$

and thus

$$t(w, t_c) = t_c + \frac{h - \int_{t_0}^{t_c} u_{fs}(t'_c) dt'_c}{w + u_{fs}(t_c)}. \quad (2.20)$$

This leads to

$$\begin{aligned} \frac{dt}{dt_c} &= 1 - \frac{u_{fs}(t_c)}{w + u_{fs}(t_c)} - u'_{fs}(t_c) \cdot \frac{h - \int_{t_0}^{t_c} u_{fs}(t'_c) dt'_c}{[w + u_{fs}(t_c)]^2} \\ &= \frac{w}{w + u_{fs}(t_c)} - u'_{fs}(t_c) \cdot \frac{h - \int_{t_0}^{t_c} u_{fs}(t'_c) dt'_c}{[w + u_{fs}(t_c)]^2}. \end{aligned} \quad (2.21)$$

When u_{fs} is constant, this reduces to Equation 2.1. When u_{fs} is decreasing, Δt increases relative to Δt_c , which matches our expectations: it is the motion of the free surface which leads to the compressed interval at the sensor relative to the source, so if the free surface becomes motionless, the source and sensor intervals will become equivalent. Conversely, if u_{fs} is increasing, then the arrival interval relative to the creation interval will become even shorter than that obtained for the case of a constant u_{fs} .

Given a known $u_{fs}(t_c)$, Equation 2.20 cannot be solved algebraically for t_c . The entire treatment for this scenario becomes nonalgebraic.

In situations where the free surface is driven by an unsupported shock (e.g., a Taylor wave), u_{fs} may indeed decrease during the ejecta creation period. However, the present formulation can still be used to estimate the errors in the piezoelectric mass measurement (see Section 3) by computing $\chi(t)$ (see Equation 3.1) for both $u_{fs} = u_{fs}(t_0)$ and $u_{fs} = \min(u_{fs})$.

3 General expression for the error in the inferred areal mass, χ

Specific test problems notwithstanding, it is very easy to derive an expression for $\chi(t)$, the ratio of the inferred accumulated areal mass to the true accumulated areal mass, for an *arbitrary* areal mass function $m_c(w, t_c)$.

Recall, from Equation 2.17, that the true accumulated areal mass at the sensor is

$$m_t(t) = \int_0^t dt' \int_0^\infty m_a(u, t') du$$

while from Equation 2.18 the inferred accumulated areal mass at the sensor is

$$\begin{aligned} m_i(t) &= \int_0^t \left(\frac{t' - t_0}{h} \right) P(t') dt' = \int_0^t dt' \left(\frac{t' - t_0}{h} \right) \int_0^\infty m_a(u, t') u du \\ &= \frac{1}{h} \int_0^t dt' \int_0^\infty m_a(u, t') u t' du, \end{aligned}$$

where for simplicity we have set $t_0 = 0$. Note the similarities between the two expressions. In subsequent sections we'll use equations derived from these expressions to compare $m_t(t)$ and $m_i(t)$ for specific test problems and several general cases. However, the most general relationship can be derived by using Equation 2.14 to write these areal masses as functions of m_c rather than m_a . When $t_0 = 0$, the true accumulated areal mass becomes

$$m_t(t) = \int_0^t dt' \int_0^\infty \left(\frac{u}{u - u_{fs}} \right) m_c \left(u - u_{fs}, \frac{ut' - h}{u - u_{fs}} \right) du.$$

Let $x \equiv u - u_{fs}$ (which is really w , but to avoid confusion for the moment we simply define x as a variable with units of velocity). Then

$$m_t(t) = \int_0^t dt' \int_{-u_{fs}}^\infty \left(\frac{x + u_{fs}}{x} \right) m_c \left[x, \frac{(x + u_{fs})t' - h}{x} \right] dx.$$

Now let $y \equiv \frac{(x + u_{fs})t' - h}{x}$. (In reality, $y = t_c(w, t')$, but for the moment we disregard that association to avoid confusion. Like x , y is simply a convenient substitution variable.) Note there is no problem with y diverging at $x = 0$: ejecta particles can

only arrive at the sensor when $u > u_{fs} \implies x > 0$ (see Section 2.4 regarding the limits of integration). Then

$$\begin{aligned} m_t(t) &= \int_{-u_{fs}}^{\infty} dx \int_{-\frac{h}{x}}^{\frac{(x+u_{fs})t-h}{x}} \left(\frac{x+u_{fs}}{x} \right) m_c(x, y) \left(\frac{x}{x+u_{fs}} \right) dy \\ &= \int_0^{\infty} dx \int_0^{t_c(x,t)} m_c(x, y) dy \end{aligned}$$

This expression makes sense. It's the integral of the areal mass function at the source over the *creation* interval that corresponds to the *arrival* interval ending at time t .

The inferred areal mass at the sensor is

$$m_i(t) = \frac{1}{h} \int_0^t dt' \int_0^{\infty} \left(\frac{u}{u - u_{fs}} \right) m_c \left(u - u_{fs}, \frac{ut' - h}{u - u_{fs}} \right) u t' du.$$

Let us apply the same substitution variables, x and y , from above. Now

$$ut' = (x + u_{fs}) \cdot \left(\frac{xy + h}{x + u_{fs}} \right) = xy + h,$$

and thus

$$\begin{aligned} m_i(t) &= \frac{1}{h} \int_{-u_{fs}}^{\infty} dx \int_{-\frac{h}{x}}^{\frac{(x+u_{fs})t-h}{x}} \left(\frac{x+u_{fs}}{x} \right) m_c(x, y) (xy + h) \left(\frac{x}{x+u_{fs}} \right) dy \\ &= \frac{1}{h} \int_0^{\infty} dx \int_0^{t_c(x,t)} m_c(x, y) (xy + h) dy \\ &= \int_0^{\infty} dx \int_0^{t_c(x,t)} m_c(x, y) dy + \frac{1}{h} \int_0^{\infty} dx \int_0^{t_c(x,t)} m_c(x, y) x y dy \\ &= m_t(t) + \frac{1}{h} \int_0^{\infty} dx \int_0^{t_c(x,t)} m_c(x, y) x y dy. \end{aligned}$$

We therefore find that for *any* given areal mass function at the source, $m_c(w, t_c)$, the ratio of inferred to true accumulated areal mass at the sensor is

$$\frac{m_i(t)}{m_t(t)} \equiv \chi(t) = 1 + \frac{1}{h} \cdot \frac{\int_0^{\infty} dx \int_0^{t_c(x,t)} m_c(x, y) x y dy}{\int_0^{\infty} dx \int_0^{t_c(x,t)} m_c(x, y) dy}$$

or

$$\chi(t) = 1 + \frac{1}{h} \cdot \frac{\int_{w_0}^{w_1} \int_0^{t_c(w,t)} w t_c m_c(w, t_c) dt_c dw}{\int_{w_0}^{w_1} \int_0^{t_c(w,t)} m_c(w, t_c) dt_c dw}$$

where $t_c(w, t) = \frac{(w+u_{fs})t-h}{w}$ and we have denoted the minimum and maximum relative velocities by w_0 and w_1 , respectively. Note $t_c(w, t_c) \geq 0 \implies w \geq \frac{h}{t} - u_{fs}$. Finally, then, we have

$$\chi(t) = 1 + \frac{1}{h} \cdot \frac{\int_{\frac{h}{t}-u_{fs}}^{w_1} \int_0^{t_c(w,t)} w t_c m_c(w, t_c) dt_c dw}{\int_{\frac{h}{t}-u_{fs}}^{w_1} \int_0^{t_c(w,t)} m_c(w, t_c) dt_c dw}.$$

(3.1)

For sufficiently large arrival times, t , (such as when evaluating the $\chi(t)$ at the end of the arrival period) the lower bound on the velocity integral will fall below w_0 , at which point it can be replaced with w_0 .

Note that Equation 3.1 is the error imposed *on a perfect system* by the assumption of instantaneous ejecta creation. The overall error in the inferred mass will be higher in a real measurement, owing to noise and other effects.

We have defined the problem such that $m_c \geq 0$, $w \geq 0$, and $t_c \geq 0$. This means $\chi(t) \geq 1$ for all arrival times t , which in turn means that for a perfect system *the piezoelectric sensor analysis can never underestimate the ejecta mass*. By assuming all particles are launched instantaneously, the piezo analysis implicitly interprets later-arriving particles as being slower but heavier to achieve the same impulse. So the analysis skews toward larger ejecta masses later in the arrival period.

If, in the chosen units, $w_1 \leq 1$ (i.e. $u_1 = u_{ej} \leq 2u_{fs}$) and $t_c(w, t) \leq 1$ for all (w, t) , then the ratio of integrals can never exceed unity, much less h .

The error percentage, P , is

$$\frac{100}{h} \cdot \frac{\int_{\frac{h}{t}-u_{fs}}^{w_1} \int_0^{t_c(w,t)} w t_c m_c(w, t_c) dt_c dw}{\int_{\frac{h}{t}-u_{fs}}^{w_1} \int_0^{t_c(w,t)} m_c(w, t_c) dt_c dw},$$

so for the error level to exceed $P\%$ requires

$$\frac{100}{hP} \cdot \int_{\frac{h}{t}-u_{fs}}^{w_1} \int_0^{t_c(w,t)} w t_c m_c(w, t_c) dt_c dw > \int_{\frac{h}{t}-u_{fs}}^{w_1} \int_0^{t_c(w,t)} m_c(w, t_c) dt_c dw. \quad (3.2)$$

Consider the quantity $\frac{100}{hP} w t_c$. If this were exactly unity over the entire integration domain, then the left and right sides of Equation 3.2 would be identically equal. If this quantity were less than unity over the entire integration domain, then the integrand of the left side would be less than the integrand of the right side at every point in the domain. Because all quantities are nonnegative for this problem, that would guarantee the quantity on the left is less than the quantity on the right. Therefore, the inequality in Equation 3.2 can only be satisfied if

$$\frac{100}{hP} w t_c > 1 \quad \text{or} \quad w t_c > \frac{hP}{100}$$

over at least some portion of the integration domain (which is a function of t).

Each P value therefore defines a curve in the (w, t_c) plane; this curve must intersect the integration domain in order for the error percentage to exceed $P\%$. (Intersection is a necessary but not sufficient condition.) Clearly then, there is a maximum error percentage, P_{max} , such that the curves for $P > P_{max}$ never intersect the integration domain. A simple estimate for P_{max} is

$$P_{max} = \max 100 \cdot \frac{w}{h} \cdot t_c$$

where the maximum is computed over the domain of integration. A straightforward value for this bound uses the maximum ejecta relative velocity, w_1 , and the final creation time, t_{cf} (or the duration of the creation interval, $t_{cf} - t_0$, if $t_0 \neq 0$). (This is an estimate because particles of velocity w_1 might not be emitted at time t_{cf} , if the velocity distribution defined by $m_c(w, t_c)$ is nonstationary.) Finally, then, the absolute upper bound on the error percentage is

$$P_{max} = 100 \cdot \frac{w_1 t_{cf}}{h}. \quad (3.3)$$

(Interestingly, this is the simplest first-order quantity that one might construct from dimensional analysis and a consideration of how the error might be expected to scale with the pin distance and creation time.) For experiments where h is known from the configuration and u_{fs} and $u_{ej} \equiv u_1 = w_1 + u_{fs}$ are measured, this sets an upper bound on the error as a function of the creation interval.

For a given arrival time, t , the integration domain is the region of the (w, t_c) plane bounded by the inequalities

$$\frac{h}{t} - u_{fs} \leq w \leq w_1 \quad 0 \leq t_c \leq \frac{(w + u_{fs})t - h}{w}.$$

The portion of this domain where $wt_c > \frac{hP}{100}$ is that part of the domain above the line $t_c = \frac{hP}{100w}$. This is represented schematically in Figure 2, as is the contour for $P = P_{max}$.

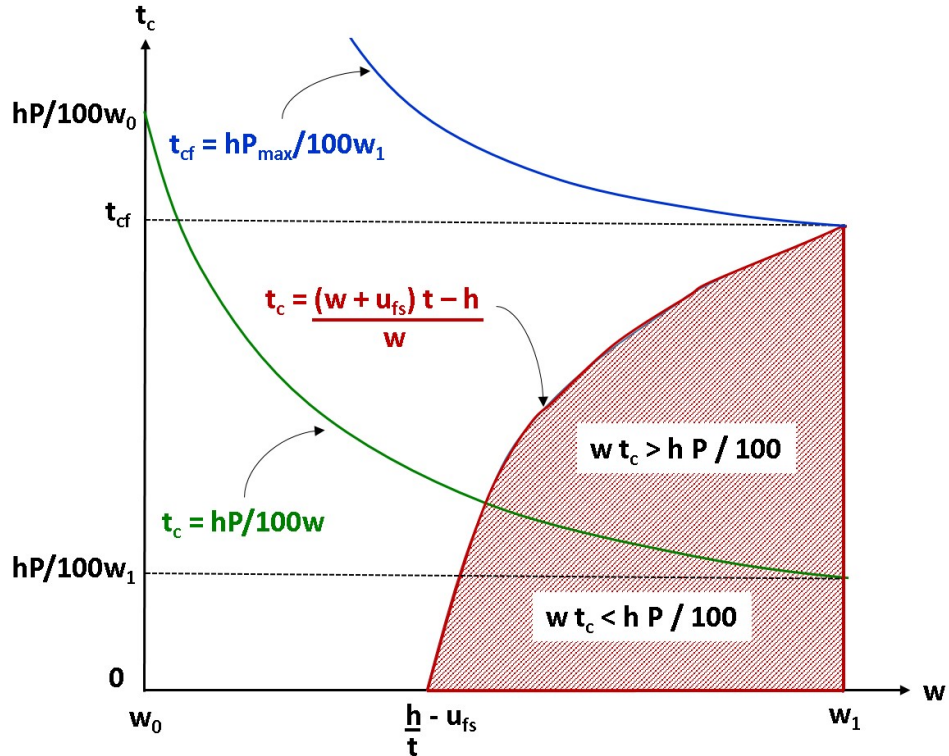


Figure 2: Cartoon depiction of the integration domain for computing $\chi(t)$. The shaded red region is the domain of integration at time t . The green line represents the boundary between $wt_c > \frac{hP}{100}$ and $wt_c < \frac{hP}{100}$ for a given error percentage, P . The error cannot exceed $P\%$ unless the green line intersects the domain of integration, as illustrated here (intersection is a necessary but not sufficient condition). The blue line represents the (w, t_c) contour for the largest possible P value, P_{max} . Note this cartoon makes no assertions about the areal mass function $m_c(w, t_c)$, only its domain of integration relevant for $\chi(t)$.

The curve $t_c = \frac{(w+u_{fs})t-h}{w}$ must be negative for $w < \frac{h}{t} - u_{fs}$ and must increase

with increasing w because $t_c \rightarrow t$ in the limit $w \rightarrow \infty$. Thus in order for the integration domain to contain points with $wt_c > \frac{hP}{100}$, the creation interval must extend to times

$$t_c > \frac{hP}{100w_1}.$$

As an example, the parameter values explored in Section 5.1 (Shot 6 of [1]) yield $\frac{h}{w_1} \approx 32.4 \mu\text{s}$, meaning the upper bound on the error will be less than 3% unless the creation interval exceeds 1 microsecond. We can also set a requirement for the arrival time, t :

$$\frac{(w_1 + u_{fs})t - h}{w_1} > \frac{hP}{100w_1} \implies t > \frac{h}{u_1} \left(1 + \frac{P}{100} \right).$$

The above parameter values yield $\frac{h}{u_1} \approx 7.5 \mu\text{s}$.

3.1 Instantaneous creation

Note that when the ejecta creation is instantaneous at the time of shock breakout, the areal mass function at the source will have the form

$$m_c(w, t_c) = g(w)\delta(t_c - t_0) = f(w)\delta(t_c)$$

when $t_0 = 0$. Because $m_c = 0$ for $t_c < 0$, the lower limit of integration over t_c may be extended to any negative value. Thus, the numerator of the second term of Equation 3.1 evaluates to zero in this case. This confirms that the piezoelectric sensor analysis is guaranteed to give the correct result (again, for a perfect system) when the creation is instantaneous.

3.2 Stationary velocity distributions

If the ejecta velocity distribution is stationary, then the areal mass function at the source can be written

$$m_c(w, t_c) = f(t_c)g(w).$$

Then the second term of Equation 3.1 becomes

$$\frac{1}{h} \cdot \frac{\int_{\frac{h}{t} - u_{fs}}^{w_1} w g(w) dw}{\int_{\frac{h}{t} - u_{fs}}^{w_1} g(w) dw} \cdot \frac{\int_0^{t_c(w,t)} t_c f(t_c) dt_c}{\int_0^{t_c(w,t)} f(t_c) dt_c}.$$

When both upper limits of integration are < 1 in the units of the problem, each integral ratio must be less than unity.

3.3 Time-dependent u_{fs}

When u_{fs} is constant, the free surface velocity enters $\chi(t)$ only via the limits of integration in Equation 3.1. If instead u_{fs} is a function of t_c , the resulting nonalgebraic formulation could be considerably different. However, in that case, the true value of $\chi(t)$ may be expected to reside in the range defined by evaluations of Equation 3.1 for the maximum and minimum values of u_{fs} over the ejecta creation period. From dimensional analysis, we expect Equation 3.3 to provide a decent estimate of P_{max} , even for this scenario.

4 Analytic test problems with stationary velocity distributions

We can now compare the true and inferred accumulated areal masses at the sensor for a variety of analytic test problems. We begin by exploring test problems where the velocity distribution at the source does not evolve during the production period. In these cases, the areal mass function at the source may be considered the product of two separable functions, one governing the time dependence and another governing the velocity dependence.

4.1 Delta function properties

In what follows, several of our analytic test problems will define the areal mass function at the free surface in terms of Dirac delta functions. Care must be taken to ensure these problems are evaluated correctly. It is therefore worthwhile to review one particular property of the delta function, which will recur in several calculations.

Our test problems will frequently involve expressions where the argument of the delta function is, itself, a function of t or u or both. In such cases, the composition of a delta function with a regular analytic function is correctly given by

$$\delta[f(x)] = \sum_i \frac{\delta(x - x_i)}{|f'(x_i)|} \quad (4.1)$$

where the x_i are zeroes of $f(x)$. It immediately follows that

$$\int_{x_1}^{x_2} g(x) \delta[f(x)] dx = \sum_i \frac{g(x_i)}{|f'(x_i)|} \quad (4.2)$$

where the sum spans those zeroes of f contained within the integration domain.

When considering expressions of the form

$$\int \cdots dt \int \cdots \delta[f(u, t)] du$$

it is helpful to consider the delta function as an object whose properties are only defined under integration. In particular, the delta function is always a function of the variable of integration. Thus, when evaluating the above expression, we should treat t as a constant and $f(u, t)$ strictly as a function of u when applying Equation 4.1 (and vice-versa if the order of integration were reversed).

4.2 TP 1: Instantaneous production, single fixed velocity

The simplest possible test problem is one where ejecta are created instantaneously at the free surface with only a single relative velocity:

$$m_c(w, t_c) = m_0 \delta(w - \bar{w}) \delta(t_c - \bar{t}) \quad (4.3)$$

where here m_0 has the units [mass · area⁻¹]. This problem is equivalent to the situation where only a single particle is ejected.

Step 1: Derive m_a

From Equation 2.14, the areal mass function at the sensor is

$$m_a(u, t) = \left(\frac{u}{u - u_{fs}} \right) m_0 \delta(u - u_{fs} - \bar{w}) \delta\left[\frac{ut - (h + u_{fs}t_0)}{u - u_{fs}} - \bar{t} \right] \quad (4.4)$$

$$= m_0 \left(\frac{u}{u - u_{fs}} \right) \delta(u - \bar{u}) \delta[f(t)] \quad (4.5)$$

where we have defined $\bar{u} \equiv \bar{w} + u_{fs}$. Note f is truly a function of both u and t , but the velocity delta function effectively sets u constant. For our current purposes, it is sufficient and correct to treat f solely as a function of t , as shown below. It is straightforward to show

$$f'(t) = \frac{u}{u - u_{fs}} \quad \text{and} \quad f(t) = 0 \implies t = t(u - u_{fs}, \bar{t})$$

where we have used Equation 2.1. From Equation 4.1, then, we know

$$\delta\left[\frac{ut - (h + u_{fs}t_0)}{u - u_{fs}} - \bar{t} \right] = \left(\frac{u - u_{fs}}{u} \right) \delta[t - t(u - u_{fs}, \bar{t})] \quad (4.6)$$

where we have dropped the absolute value brackets because all lab-frame ejecta velocities must be greater than the free surface velocity. Finally, then, the areal mass function at the sensor is simply

$$m_a(u, t) = m_0 \delta(u - \bar{u}) \delta[t - t(u - u_{fs}, \bar{t})]. \quad (4.7)$$

Step 2: Confirm m_a by testing mass conservation

The total ejected areal mass at the free surface is

$$\int_0^\infty \int_0^\infty m_0 \delta(w - \bar{w}) \delta(t_c - \bar{t}) dw dt_c = m_0.$$

The total areal mass received at the sensor is

$$\int_0^\infty \int_0^\infty m_0 \delta(u - \bar{u}) \delta[t - t(u - u_{fs}, \bar{t})] du dt = m_0 \int_0^\infty \delta[t - t(\bar{u} - u_{fs}, \bar{t})] dt$$

but $t(\bar{u} - u_{fs}, \bar{t})$ is, by definition, the arrival time for a particle of relative velocity \bar{w} launched at time \bar{t} . All ejecta particles share that velocity and launch time so there is only one arrival time in the problem. So let us denote $t(\bar{u} - u_{fs}, \bar{t}) \equiv \bar{t}^a$. Then the total received areal mass becomes

$$m_0 \int_0^\infty \delta(t - \bar{t}^a) dt = m_0,$$

which proves that mass is conserved and our expression for m_a is correct.

Step 3: Compute pressure at the surface and the pin

The pressure at the free surface is simply

$$P_c(t_c) = \int_0^\infty m_c(w, t_c) w dw = \int_0^\infty m_0 w \delta(w - \bar{w}) \delta(t_c - \bar{t}) = m_0 \bar{w} \delta(t_c - \bar{t}).$$

This quantity has the units of momentum flux, and it is impulsive, as expected.

The pressure on the pin is

$$P(t) = \int_0^\infty m_a(u, t) u du = \int_0^\infty m_0 u \delta(u - \bar{u}) \delta[t - t(u - u_{fs}, \bar{t})] du$$

$$= m_0 \bar{u} \delta(t - \bar{t}^a).$$

Again this is impulsive, but now the pressure at the pin (in the instant of arrival) is $\frac{\bar{u}}{\bar{w}}$ times the pressure at the surface (in the instant of creation). This is consistent with expectations, because the free surface sees a particle with velocity \bar{w} but the pin sees a particle with velocity \bar{u} , and the pressure is derived from the momentum flux. Because the ejection and arrival are both instantaneous in this problem, the time contraction of the arrival interval relative to the creation interval does not come into play (see test problem 2, below).

Step 4: Compare the true and inferred accumulated areal masses

The *true* accumulated areal mass at the pin is

$$\begin{aligned} m_t(t) &= \int_0^t \int_0^\infty m_a(u, t') du dt' \\ &= \int_0^t \int_0^\infty m_0 \delta(u - \bar{u}) \delta[t' - t(u - u_{fs}, \bar{t})] du dt' \\ &= \int_0^t \delta[t' - t(\bar{u} - u_{fs}, \bar{t})] dt' \\ &= m_0 \int_0^t \delta(t' - \bar{t}^a) dt' \\ &= \begin{cases} 0 & t < \bar{t}^a \\ m_0 & t > \bar{t}^a \end{cases}. \end{aligned}$$

This is exactly what we expect based on dimensional analysis and the observation that the arrival is instantaneous.

The definition of this test problem implicitly assumes $\bar{t} = t_0$. So the *inferred* accumulated areal mass at the source is

$$\begin{aligned} m_i(t) &= \int_0^t \left(\frac{t' - \bar{t}}{h} \right) P(t') dt' \\ &= \int_0^t \left(\frac{t' - \bar{t}}{h} \right) m_0 \bar{u} \delta(t' - \bar{t}^a) dt' \\ &= \left(\frac{m_0 \bar{u}}{h} \right) \int_0^t (t' - \bar{t}) \delta(t' - \bar{t}^a) dt' \end{aligned}$$

$$= \begin{cases} 0 & t < \bar{t}^a \\ \frac{m_0 \bar{u}}{h} (\bar{t}^a - \bar{t}) & t > \bar{t}^a \end{cases}.$$

But $\bar{t}^a - \bar{t}$ is simply the interval between the ejection and arrival times, and that is simply the time of flight for the ejected particle. Indeed,

$$\bar{t}^a - \bar{t} = t(\bar{u} - u_{fs}, \bar{t}) - \bar{t} = \bar{t} + \frac{h - u_{fs}(\bar{t} - \bar{t})}{\bar{u}} - \bar{t} = \frac{h}{\bar{u}}$$

and therefore the inferred areal mass at the pin is

$$m_i(t) = \begin{cases} 0 & t < \bar{t}^a \\ m_0 & t > \bar{t}^a \end{cases}.$$

Thus, for the case where ejecta particles are produced instantaneously with a single velocity, the true and inferred accumulated areal masses agree. This is as it should be, because the assumption underlying this test problem (instantaneous ejecta production) also underlies the piezoelectric sensor analysis. Furthermore, we find the formalism derived in Section 2 produces the correct answers for this test problem.

4.3 TP 2: Sustained production, single fixed velocity

Now consider the case where the ejecta are still created with only a single velocity, but over a sustained time interval (i.e., the ejecta are no longer created impulsively at shock breakout). Let the creation interval persist from t_0 (the shock breakout at the free surface) to t_1 . Then

$$m_c(t_c, w) = m_0 \delta(w - \bar{w}) \Pi_{t_0}^{t_1}(t_c), \quad (4.8)$$

where we use Π to denote a boxcar function. The units of m_0 are [mass · area⁻¹ · time⁻¹].

Step 1: Derive m_a

From Equation 2.14 the areal mass function at the sensor is

$$m_a(u, t) = \left(\frac{u}{u - u_{fs}} \right) m_0 \delta(u - u_{fs} - \bar{w}) \Pi_{t_0}^{t_1} \left[\frac{ut - (h + u_{fs}t_0)}{u - u_{fs}} \right].$$

The boxcar function is nonzero for

$$t_0 < \frac{ut - (h + u_{fs}t_0)}{u - u_{fs}} < t_1$$

or

$$\frac{(u - u_{fs})t_0 + h + u_{fs}t_0}{u} < t < \frac{(u - u_{fs})t_1 + h + u_{fs}t_0}{u}$$

or simply

$$t(w = u - u_{fs}, t_0) < t < t(w = u - u_{fs}, t_1).$$

If we denote the arrival time for particles emitted at time t_0 by $t_0^a(u) \equiv t(w = u - u_{fs}, t_0)$ and the arrival time for particles emitted at t_1 by $t_1^a(u) \equiv t(w = u - u_{fs}, t_1)$, then the areal mass function at the sensor can be written

$$m_a(u, t) = m_0 \left(\frac{u}{u - u_{fs}} \right) \delta(u - \bar{u}) \prod_{t_0^a(u)}^{t_1^a(u)} (t) \quad (4.9)$$

where again we have defined $\bar{u} = \bar{w} + u_{fs}$.

Step 2: Confirm m_a by testing mass conservation

The total areal mass created at the free surface is

$$\begin{aligned} \int_0^\infty \int_0^\infty m_c(w, t_c) dw dt_c &= \int_0^\infty \int_0^\infty m_0 \delta(w - \bar{w}) \prod_{t_0}^{t_1} (t_c) dw dt_c \\ &= m_0 (t_1 - t_0) \\ &= m_0 \Delta t_c. \end{aligned}$$

The total areal mass received at the sensor is

$$\begin{aligned} \int_0^\infty \int_0^\infty m_a(u, t) du dt &= \int_0^\infty \int_0^\infty m_0 \left(\frac{u}{u - u_{fs}} \right) \delta(u - \bar{u}) \prod_{t_0^a(u)}^{t_1^a(u)} (t) du dt \\ &= m_0 \left(\frac{\bar{u}}{\bar{u} - u_{fs}} \right) [t_1^a(\bar{u}) - t_0^a(\bar{u})] \\ &= m_0 \left(\frac{\bar{u}}{\bar{u} - u_{fs}} \right) \Delta t \\ &= m_0 \left(\frac{\bar{u}}{\bar{u} - u_{fs}} \right) \left(\frac{\bar{u} - u_{fs}}{\bar{u}} \right) \Delta t_c \\ &= m_0 \Delta t_c. \end{aligned}$$

This confirms that mass is conserved and our expression for m_a is correct.

Step 3: Compute pressure at the surface and the pin

The pressure on the free surface is

$$P_c(t_c) = \int_0^\infty m_c(w, t_c) w dw = \int_0^\infty m_0 w \delta(w - \bar{w}) \prod_{t_0}^{t_1}(t_c) dw = m_0 \bar{w} \prod_{t_0}^{t_1}(t_c).$$

The units are correct. The free surface experiences a recoil pressure (momentum) only while it is launching ejecta.

The pressure on the sensor is

$$\begin{aligned} P(t) &= \int_0^\infty m_a(u, t) u du = \int_0^\infty m_0 \left(\frac{u^2}{u - u_{fs}} \right) \delta(u - \bar{u}) \prod_{t_0^a(u)}^{t_1^a(u)}(t) du \\ &= m_0 \left(\frac{\bar{u}^2}{\bar{u} - u_{fs}} \right) \prod_{t_0^a(\bar{u})}^{t_1^a(\bar{u})}(t) \\ &= m_0 \left(\frac{\bar{u}^2}{\bar{w}} \right) \prod_{t_0^a(\bar{u})}^{t_1^a(\bar{u})}(t). \end{aligned}$$

We find the instantaneous pressure on the pin during the arrival interval is larger than the instantaneous pressure on the free surface during the ejection interval by a factor of $(\frac{\bar{u}}{\bar{w}})^2$. One factor of the velocity ratio comes from the velocity shift between the free-surface and lab (sensor) frames. We observed this in the previous test problem, where ejecta creation was instantaneous. Now a second factor of the velocity ratio enters the problem, owing to the relative time contraction of the arrival interval at the sensor compared to the creation interval at the free surface.

Step 4: Compare the true and inferred accumulated areal masses

The *true* accumulated areal mass at the pin is

$$\begin{aligned} m_t(t) &= \int_0^t \int_0^\infty m_a(u, t') du dt' \\ &= \int_0^t \int_0^\infty m_0 \left(\frac{u}{u - u_{fs}} \right) \delta(u - \bar{u}) \prod_{t_0^a(u)}^{t_1^a(u)}(t) du dt' \\ &= m_0 \int_0^\infty \left(\frac{u}{u - u_{fs}} \right) \delta(u - \bar{u}) \int_0^t \prod_{t_0^a(u)}^{t_1^a(u)}(t) dt du \end{aligned}$$

$$= m_0 \left(\frac{\bar{u}}{\bar{u} - u_{fs}} \right) \cdot \begin{cases} 0 & t \leq t_0^a < t_1^a \\ t - t_0^a & t_0^a \leq t \leq t_1^a \\ t_1^a - t_0^a & t_0^a < t_1^a \leq t \end{cases}$$

where we have defined $t_0^a \equiv t_0^a(\bar{u})$ and $t_1^a \equiv t_1^a(\bar{u})$. Note $t_1^a - t_0^a = \Delta t = \left(\frac{\bar{w}}{\bar{u}}\right) \Delta t_c$, so the true accumulated areal mass at the pin can be written

$$m_t(t) = m_0 \cdot \begin{cases} 0 & t \leq t_0^a < t_1^a \\ \left(\frac{\bar{u}}{\bar{w}}\right) (t - t_0^a) & t_0^a \leq t \leq t_1^a \\ \Delta t_c & t_0^a < t_1^a \leq t \end{cases}$$

The units are correct. The true accumulated mass increases linearly with time, as we might expect.

The *inferred* accumulated areal mass at the pin is

$$\begin{aligned} m_i(t) &= \int_0^t \left(\frac{t' - t_0}{h} \right) P(t') dt' \\ &= \int_0^t \left(\frac{t' - t_0}{h} \right) m_0 \left(\frac{\bar{u}^2}{\bar{w}} \right) \prod_{t_0^a(\bar{u})}^{t_1^a(\bar{u})} (t') dt' \\ &= \frac{m_0 \bar{u}^2}{h \bar{w}} \cdot \begin{cases} 0 & t \leq t_0^a < t_1^a \\ \int_{t_0^a}^t (t' - t_0) dt' & t_0^a \leq t \leq t_1^a \\ \int_{t_0^a}^{t_1^a} (t' - t_0) dt' & t_0^a < t_1^a \leq t \end{cases} \end{aligned}$$

or

$$m_i(t) = \frac{m_0 \bar{u}^2}{h \bar{w}} \cdot \begin{cases} 0 & t \leq t_0^a < t_1^a \\ (t - t_0^a) \left[\frac{t + t_0^a}{2} - t_0 \right] & t_0^a \leq t \leq t_1^a \\ (t_1^a - t_0^a) \left[\frac{t_1^a + t_0^a}{2} - t_0 \right] & t_0^a < t_1^a \leq t \end{cases}$$

Again using $t_1^a - t_0^a = \Delta t = \left(\frac{\bar{w}}{\bar{u}}\right) \Delta t_c$, we can write this as

$$m_i(t) = m_0 \cdot \begin{cases} 0 & t \leq t_0^a < t_1^a \\ \frac{\bar{u}^2}{h \bar{w}} \cdot (t - t_0^a) \left[\frac{t + t_0^a}{2} - t_0 \right] & t_0^a \leq t \leq t_1^a \\ \Delta t_c \cdot \frac{\bar{u}}{h} \left[\frac{t_1^a + t_0^a}{2} - t_0 \right] & t_0^a < t_1^a \leq t \end{cases}$$

The units are correct. But now we find *the inferred accumulated areal mass is a quadratic function of time during the arrival interval, whereas the true areal mass depends linearly on time during the arrival interval*. The disagreement is not surprising, because this test problem violates the assumption of instantaneous ejecta creation which underlies the piezoelectric sensor analysis.

The inferred areal mass at the final time of collection will overestimate the true areal mass at that time by a factor of

$$\frac{\bar{u}}{h} \left[\frac{t_1^a + t_0^a}{2} - t_0 \right].$$

The bracketed quantity is the time interval from shock breakout to the middle of the arrival interval. As the arrival interval becomes infinitesimally short, the bracketed quantity becomes the time of flight, or simply $\frac{h}{\bar{u}}$, and the ratio of final inferred to final true areal mass will approach 1.

We might wonder when the true and inferred areal masses agree. At that time, t^* ,

$$m_0 \frac{\bar{u}^2}{h\bar{w}} \cdot (t^* - t_0^a) \left[\frac{t^* + t_0^a}{2} - t_0 \right] = m_0 \left(\frac{\bar{u}}{\bar{w}} \right) (t^* - t_0^a)$$

or

$$\frac{\bar{u}}{h} \left[\frac{t^* + t_0^a}{2} - t_0 \right] = 1.$$

or

$$t^* = 2 \left(t_0 + \frac{h}{\bar{u}} \right) - t_0^a = 2t_0^a - t_0^a = t_0^a.$$

In other words, the true and inferred areal masses will only agree up to the first instant of ejecta arrival (i.e., while the accumulated areal mass is 0). Subsequent to the onset of ejecta arrival at the sensor, the inferred areal mass will always be larger than the true areal mass.

Consider a typical experimental case, such as Shot 6 from [1]. There the pin distance was $h = 18.57$ mm, the free surface velocity was $u_{fs} = 1.91$ mm/ μ s, and the maximum ejecta velocity was approximately $1.3u_{fs}$. Using $\bar{u} = 1.3u_{fs}$ and an ejecta creation interval of 150 ns, we get

$$\frac{\bar{u}}{h} \left[\frac{t_1^a + t_0^a}{2} - t_0 \right] \approx 1.00231.$$

(Equation 3.3 gives an upper bound on the error of 0.46% when the creation interval is 150 ns.) If we increase \bar{u} to twice the free surface velocity, the error factor increases insignificantly to 1.00771. If $\bar{u} = 1.3u_{fs}$ and the ejection interval is allowed to persist for a full microsecond, the error factor is still only 1.01543, or 1.5% (compared to an upper bound of $\sim 3.1\%$, via Equation 3.3).

4.4 TP 3: Instantaneous production, power law velocity distribution

The preceding test problems examined cases where the ejecta are produced with a single velocity. Experimental observations show this is not the case. Next, let us examine a case where the production is instantaneous but the ejecta are born with a power-law distribution of velocities:

$$m_c(w, t_c) = \begin{cases} m_0 \delta(t_c - t_0) \left(\frac{w}{w_0}\right)^{-\alpha} & w_1 \leq w \leq w_2 \\ 0 & w < w_1, w > w_2 \end{cases} \quad (4.10)$$

The units on m_0 are [mass \cdot area $^{-1}$ \cdot velocity $^{-1}$].

Step 1: Derive m_a

The areal mass function at the sensor is

$$\begin{aligned} m_a(u, t) &= \left(\frac{u}{u - u_{fs}}\right) m_c \left[u - u_{fs}, \frac{ut - (h + u_{fs}t_0)}{u - u_{fs}} \right] \\ &= \left(\frac{u}{u - u_{fs}}\right) \frac{m_0 w_0^\alpha}{(u - u_{fs})^\alpha} \delta \left[\frac{ut - (h + u_{fs}t_0)}{u - u_{fs}} - t_0 \right] \\ &= m_0 w_0^\alpha \frac{u}{(u - u_{fs})^{1+\alpha}} \delta[f(t)] \\ &= \frac{m_0 w_0^\alpha}{(u - u_{fs})^\alpha} \delta[t - t(u - u_{fs}, t_0)] \end{aligned} \quad (4.11)$$

where we have used the form of $\delta[f(t)]$ derived in Section 4.2.

Step 2: Confirm m_a by testing mass conservation

The total ejected areal mass is

$$\begin{aligned} \int_0^\infty \int_0^\infty m_c(w, t_c) dw dt_c &= m_0 w_0^\alpha \int_{w_1}^{w_2} w^{-\alpha} dw \int_0^\infty \delta(t_c - t_0) dt_c \\ &= m_0 w_0^\alpha \left(\frac{w_2^{1-\alpha} - w_1^{1-\alpha}}{1-\alpha} \right) \end{aligned}$$

and the total received areal mass at the sensor is

$$\int_0^\infty \int_0^\infty m_a(u, t) du dt = m_0 w_0^\alpha \int_{w_1+u_{fs}}^{w_2+u_{fs}} (u - u_{fs})^{-\alpha} du \int_0^\infty \delta[t - t(u - u_{fs}, t_0)] dt.$$

The argument of the delta function is constant for a fixed value of u , so the total received mass at the sensor is simply

$$m_0 w_0^\alpha \int_{w_1+u_{fs}}^{w_2+u_{fs}} (u - u_{fs})^{-\alpha} du = m_0 w_0^\alpha \left(\frac{w_2^{1-\alpha} - w_1^{1-\alpha}}{1-\alpha} \right)$$

thus confirming the total ejected and received masses agree.

Step 3: Compute pressure at the surface and the pin

The pressure at the free surface is

$$\begin{aligned} P_c(t_c) &= \int_0^\infty m_c(w, t_c) w dw = m_0 w_0^\alpha \delta(t_c - t_0) \int_{w_1}^{w_2} w^{1-\alpha} dw \\ &= m_0 w_0^\alpha \left(\frac{w_2^{2-\alpha} - w_1^{2-\alpha}}{2-\alpha} \right) \delta(t_c - t_0). \end{aligned}$$

Notice how the pressure at the source is impulsive, as expected.

Meanwhile, the pressure at the pin is given by

$$P(t) = \int_0^\infty m_a(u, t) u du = m_0 w_0^\alpha \int_{u_1}^{u_2} \frac{u}{(u - u_{fs})^\alpha} \delta[t - t(u - u_{fs}, t_0)] du$$

where we have defined $u_{1,2} \equiv w_{1,2} + u_{fs}$. Now the argument of the delta function must be treated as a function of u . From Section 4.6 (see below), we know

$$\delta[t - t(u - u_{fs}, t_0)] = \frac{h}{(t - t_0)^2} \delta[u - u(t, t_0)],$$

so the pressure at the pin becomes

$$m_0 w_0^\alpha \int_{u_1}^{u_2} \frac{u}{(u - u_{fs})^\alpha} \frac{h}{(t - t_0)^2} \delta[u - u(t, t_0)] du.$$

As long as t resides within the arrival interval, i.e. as long as

$$t_1^a \equiv t(w_2, t_0) \leq t \leq t(w_1, t_0) \equiv t_2^a$$

then $u_1 \leq u(t, t_0) \leq u_2$. Finally, then, the pressure at the pin is

$$P(t) = \begin{cases} m_0 w_0^\alpha \frac{h}{(t - t_0)^2} \frac{\bar{u}}{(\bar{u} - u_{fs})^\alpha} & t_1^a \leq t \leq t_2^a \\ 0 & \text{else} \end{cases}$$

where we have denoted $\bar{u} \equiv u(t, t_0)$. Notice how the pressure at the sensor is *not* impulsive, because the distribution of velocities created at the free surface at t_0 means the ejecta arrive at the pin over a finite interval.

Step 4: Compare the true and inferred accumulated areal masses

The true accumulated areal mass at the sensor is

$$\begin{aligned} m_t(t) &= \int_0^t dt' \int_0^\infty du m_a(u, t') = m_0 w_0^\alpha \int_{t_1^a}^t dt' \int_{u_1}^{u_2} \frac{h}{(t - t_0)^2} \frac{1}{(u - u_{fs})^\alpha} \delta[u - u(t', t_0)] du \\ &= m_0 w_0^\alpha h \int_{t_1^a}^t [u(t', t_0) - u_{fs}]^{-\alpha} (t' - t_0)^{-2} dt'. \end{aligned}$$

Now

$$u(t, t_0) - u_{fs} = \frac{h}{t - t_0} - u_{fs} = \frac{h - u_{fs}(t - t_0)}{t - t_0}$$

and

$$[u(t, t_0) - u_{fs}]^{-\alpha} (t - t_0)^{-2} = \left[\frac{h - u_{fs}(t - t_0)}{t - t_0} \right]^{-\alpha} (t - t_0)^{-2} = [h - u_{fs}(t - t_0)]^{-\alpha} (t - t_0)^{\alpha - 2},$$

so the true accumulated areal mass becomes

$$m_t(t) = m_0 w_0^\alpha h \int_{t_1^a}^t \frac{(t' - t_0)^{\alpha - 2}}{[h - u_{fs}(t' - t_0)]^\alpha} dt' \tag{4.12}$$

$$\begin{aligned}
&= m_0 w_0^\alpha h \left\{ \frac{1}{h(\alpha-1)} \left[\frac{t' - t_0}{h - u_{fs}(t' - t_0)} \right]^{\alpha-1} \right\}_{t_1^a}^t \\
&= \begin{cases} \frac{m_0 w_0^\alpha}{(\alpha-1)} \left\{ \left[\frac{t - t_0}{h - u_{fs}(t - t_0)} \right]^{\alpha-1} - \left[\frac{t_1^a - t_0}{h - u_{fs}(t_1^a - t_0)} \right]^{\alpha-1} \right\} & t_1^a \leq t \leq t_2^a \\ 0 & \text{otherwise} \end{cases}.
\end{aligned}$$

The inferred areal density at the sensor is

$$\begin{aligned}
m_i(t) &= \int_0^t \left(\frac{t' - t_0}{h} \right) P(t') dt' = \int_{t_1^a}^t \left(\frac{t' - t_0}{h} \right) m_0 w_0^\alpha \frac{h}{(t' - t_0)^2} \frac{\bar{u}}{(\bar{u} - u_{fs})^\alpha} dt' \\
&= m_0 w_0^\alpha \int_{t_1^a}^t \frac{\bar{u}(t' - t_0)^{-1}}{(\bar{u} - u_{fs})^\alpha} dt'.
\end{aligned}$$

Since $\bar{u} = u(t, t_0) = \frac{h}{t - t_0}$, we have

$$\begin{aligned}
\frac{\bar{u}(t - t_0)^{-1}}{(\bar{u} - u_{fs})^\alpha} &= \frac{h}{(t - t_0)^2} \frac{1}{\left[\frac{h}{t - t_0} - u_{fs} \right]^\alpha} = \frac{h}{(t - t_0)^2} \frac{(t - t_0)^\alpha}{[h - u_{fs}(t - t_0)]^\alpha} \\
&= h \frac{(t - t_0)^{\alpha-2}}{[h - u_{fs}(t - t_0)]^\alpha}
\end{aligned}$$

and thus

$$m_i(t) = m_0 w_0^\alpha h \int_{t_1^a}^t \frac{(t' - t_0)^{\alpha-2}}{[h - u_{fs}(t' - t_0)]^\alpha} dt'.$$

At this point we have recovered expression 4.12 for the true accumulated areal mass, $m_t(t)$. So again, we find the true and inferred accumulated areal masses are identical when the ejecta are created instantaneously, even for the case of a power-law velocity distribution.

4.5 TP 4: RMI source model, single fixed velocity

Now consider the case, inspired by the Richtmyer-Meshkov instability-based ejecta source model [4, 5, 6],

$$m_c(w, t_c) = \frac{2}{3} m_0 \frac{\delta(w - \bar{w})}{t_c + \beta\tau}. \quad (4.13)$$

The constant m_0 has units [mass · area⁻¹].

Step 1: Derive m_a

The areal mass function at the sensor is

$$\begin{aligned}
m_a(u, t) &= \left(\frac{u}{u - u_{fs}} \right) m_c \left[u - u_{fs}, \frac{ut - (h + u_{fs}t_0)}{u - u_{fs}} \right] \\
&= \frac{2}{3} m_0 \left(\frac{u}{u - u_{fs}} \right) \frac{\delta(u - u_{fs} - \bar{w})}{\frac{ut - (h + u_{fs}t_0)}{u - u_{fs}} + \beta\tau} \\
&= \frac{2}{3} m_0 \delta(u - \bar{u}) \frac{u}{ut - h + \beta\tau(u - u_{fs})} \tag{4.14}
\end{aligned}$$

where for simplicity we have taken $t_0 = 0$, and we have defined $\bar{u} \equiv \bar{w} + u_{fs}$.

Step 2: Confirm m_a by testing mass conservation

To test mass conservation, we must take care to tally the ejecta mass over equivalent intervals. Let the ejecta creation interval range from t_0 to t_c : $\Delta t_c \equiv t_c - t_0 = t_c$. Then the associated arrival times are given by $t_0^a = t(\bar{w}, t_0)$ and $t_c^a = t(\bar{w}, t_c)$. From Equation 2.1, this yields

$$t_0^a = \frac{h}{\bar{u}} \quad \text{and} \quad t_c^a = t_0^a + \left(\frac{\bar{u} - u_{fs}}{\bar{u}} \right) \Delta t_c = t_0^a + \left(\frac{\bar{w}}{\bar{u}} \right) \Delta t_c = t_0^a + \Delta t.$$

Then the cumulative ejected areal mass is given by

$$\int_{t_0}^{t_c} dt' \int_0^\infty dw m_c(w, t'_c) = \frac{2}{3} m_0 \int_0^{t_c} \frac{dt'_c}{t'_c + \beta\tau} = \frac{2}{3} m_0 \ln \left(1 + \frac{t_c}{\beta\tau} \right).$$

The cumulative received areal mass over the equivalent interval is

$$\begin{aligned}
\int_{t_0^a}^{t_c^a} dt \int_0^\infty du m_a(u, t) &= \frac{2}{3} m_0 \int_{t_0^a}^{t_c^a} \frac{\bar{u}}{\bar{u}t - h + \beta\tau(\bar{u} - u_{fs})} dt \\
&= \frac{2}{3} m_0 \int_{t_0^a}^{t_c^a} \frac{dt}{t - \frac{h - \beta\tau(\bar{u} - u_{fs})}{\bar{u}}} = \frac{2}{3} m_0 \ln \left[t - \frac{h - \beta\tau(\bar{u} - u_{fs})}{\bar{u}} \right]_{t_0^a}^{t_c^a} \\
&= \frac{2}{3} m_0 \ln \left[t - \frac{h}{\bar{u}} + \frac{\beta\tau\bar{w}}{\bar{u}} \right]_{\frac{h}{\bar{u}}}^{\frac{h}{\bar{u}} + \Delta t} = \frac{2}{3} m_0 \left\{ \ln \left[\Delta t + \frac{\beta\tau\bar{w}}{\bar{u}} \right] - \ln \left[\frac{\beta\tau\bar{w}}{\bar{u}} \right] \right\}
\end{aligned}$$

$$= \frac{2}{3} m_0 \ln \left(1 + \frac{t_c}{\beta\tau} \right).$$

This confirms that mass is conserved over equivalent intervals, indicating that our expression for m_a is correct.

Step 3: Compute pressure at the surface and the pin

The pressure at the free surface is

$$P_c(t_c) = \int_0^\infty m_c(w, t_c) w \, dw = \frac{2}{3} m_0 \int_0^\infty \frac{w \delta(w - \bar{w})}{t_c + \beta\tau} \, dw = \frac{2}{3} \frac{m_0 \bar{w}}{t_c + \beta\tau}$$

and the pressure at the pin for some time $t^a > t_0^a$ is given by

$$\begin{aligned} P(t^a) &= \int_0^\infty m_a(u, t^a) u \, du = \frac{2}{3} m_0 \int_0^\infty \frac{u^2 \delta(u - \bar{u})}{ut^a - h + \beta\tau(u - u_{fs})} \, du \\ &= \frac{2}{3} \frac{m_0 \bar{u}^2}{\bar{u}t^a - h + \beta\tau(u - u_{fs})} = \frac{2}{3} \frac{m_0 \bar{u}^2}{\bar{u}t^a - (h - \beta\tau\bar{w})} \end{aligned}$$

When $t^a > t_0^a = \frac{h}{\bar{u}}$, the denominator is always positive.

Note that the voltage at the piezoelectric pin sensor for $t^a > t_0^a$ will always be negative, and will asymptotically approach 0:

$$V(t^a) = A R S \frac{dP}{dt^a} = -\frac{2}{3} A R S \frac{m_0 \bar{u}^3}{[\bar{u}t^a - (h - \beta\tau\bar{w})]^2}.$$

This represents the fact that the pressure on the pin is greatest at the first instant of ejecta arrival, after which it declines monotonically.

Step 4: Compare the true and inferred accumulated areal masses

From above, the true accumulated areal mass at the sensor for some time $t > t_0^a \equiv \frac{h}{\bar{u}}$ is given by

$$\begin{aligned} m_t(t) &= \frac{2}{3} m_0 \ln \left[t - \frac{h}{\bar{u}} + \frac{\beta\tau\bar{w}}{\bar{u}} \right]_{\frac{h}{\bar{u}}}^t = \frac{2}{3} m_0 \left\{ \ln \left[t - \frac{h}{\bar{u}} + \frac{\beta\tau\bar{w}}{\bar{u}} \right] - \ln \left[\frac{\beta\tau\bar{w}}{\bar{u}} \right] \right\} \\ &= \frac{2}{3} m_0 \ln \left[1 + \frac{t - \frac{h}{\bar{u}}}{\frac{\beta\tau\bar{w}}{\bar{u}}} \right] = \frac{2}{3} m_0 \ln \left[1 + \left(\frac{\bar{u}}{\bar{w}} \right) \frac{t - t_0^a}{\beta\tau} \right]. \end{aligned}$$

The inferred accumulated areal mass at the sensor is

$$\begin{aligned}
m_i(t) &= \int_{t_0^a}^t \left(\frac{t' - t_0}{h} \right) P(t') dt' = \frac{2}{3} \frac{m_0}{h} \int_{t_0^a}^t \frac{t' \bar{u}^2}{\bar{u}t' - h + \beta\tau\bar{w}} dt' \\
&= \frac{2}{3} \frac{m_0 \bar{u}}{h} \int_{t_0^a}^t \frac{t' dt'}{t' - \left(\frac{h - \beta\tau\bar{w}}{\bar{u}} \right)} dt' \\
&= \frac{2}{3} \frac{m_0 \bar{u}}{h} \left\{ \left(\frac{h - \beta\tau\bar{w}}{\bar{u}} \right) \ln \left[t' - \left(\frac{h - \beta\tau\bar{w}}{\bar{u}} \right) \right] + t' \right\}_{t_0^a}^t \\
&= \frac{2}{3} \frac{m_0 \bar{u}}{h} \left\{ \left(\frac{h - \beta\tau\bar{w}}{\bar{u}} \right) \ln \left[\frac{t - \left(\frac{h - \beta\tau\bar{w}}{\bar{u}} \right)}{t_0^a - \left(\frac{h - \beta\tau\bar{w}}{\bar{u}} \right)} \right] + (t - t_0^a) \right\} \\
&= \frac{2}{3} \frac{m_0 \bar{u}}{h} \left\{ \left(\frac{h - \beta\tau\bar{w}}{\bar{u}} \right) \ln \left[\frac{\bar{u}}{\bar{w}\beta\tau} \left(t - \frac{h - \beta\tau\bar{w}}{\bar{u}} \right) \right] + (t - t_0^a) \right\} \\
&= \frac{2}{3} m_0 \left\{ \left(1 - \frac{\beta\tau\bar{w}}{h} \right) \ln \left[1 + \left(\frac{\bar{u}}{\bar{w}} \right) \frac{t - t_0^a}{\beta\tau} \right] + \frac{\bar{u}}{h} (t - t_0^a) \right\}
\end{aligned}$$

Note how the expression for $m_i(t)$ contains $m_t(t)$ as well as an additional term that is linear in time.

Consider a typical case, such as Shot 6 from [1]. There the pin distance was $h = 18.57$ mm, the free surface velocity was $u_{fs} = 1.91$ mm/ μ s, and the maximum ejecta velocity was approximately $1.3u_{fs}$, so we use $\bar{u} = 1.3u_{fs}$ in this sample calculation. For this shot, $\beta \approx 1.56$ and typical τ values in a FLAG calculation for this shot ranged between 6.7 and 11.6, so we use $\beta\tau = 10$ ns for simplicity. Using the density of unshocked tin and the RMI source model (see [4, 5, 6]), the areal mass constant m_0 for this shot was approximately 1.28×10^{-3} g \cdot cm $^{-2}$.

When the ejecta creation interval persists for 150 ns, the final inferred areal mass is only a factor of 0.136% larger than the final true areal mass at the sensor. (The upper bound derived from these parameters via Equation 3.3 is 0.46%.) For a 1 μ s creation interval, the error factor is 0.638% (with an upper bound of $\sim 3.1\%$). Even with an extremely long (possibly unphysical) production interval of 10 μ s, the error factor is only 1.04435, or 4.4%. (Equation 3.3 gives only a very loose upper bound for this scenario, $\sim 31\%$.) A 10% error requires a production interval of ~ 25 μ s.

4.6 General case: Instantaneous production

The results from Sections 4.2 and 4.4, the latter in particular, reinforce the assertion that the piezoelectric analysis procedure should produce the correct (analytic) areal mass whenever the ejecta production is instantaneous. We can investigate this by examining an areal mass function with the general form

$$m_c(w, t_c) = f(w) \delta(t_c - t_0). \quad (4.15)$$

Any areal mass function m_c will have this form when the ejecta production occurs instantaneously at the moment of shock breakout.

Step 1: Derive m_a

From Equation 2.14 the areal mass function at the sensor is

$$\begin{aligned} m_a(u, t) &= \left(\frac{u}{u - u_{fs}} \right) m_c \left[u - u_{fs}, \frac{ut - (h + u_{fs}t_0)}{u - u_{fs}} \right] \\ &= \left(\frac{u}{u - u_{fs}} \right) f(u - u_{fs}) \delta \left[\frac{ut - (h + u_{fs}t_0)}{u - u_{fs}} - t_0 \right] \\ &= \left(\frac{u}{u - u_{fs}} \right) f(u - u_{fs}) \left(\frac{u - u_{fs}}{u} \right) \delta[t - t(u - u_{fs}, t_0)] \\ &= f(u - u_{fs}) \delta[t - t(u - u_{fs}, t_0)] \end{aligned} \quad (4.16)$$

where we have used Equation 4.6 (see Section 4.2). Note however the argument of the delta function may also be considered a function of u :

$$\delta[t - t(u - u_{fs}, t_0)] \equiv \delta[g(u)]$$

where

$$g(u) = t - \frac{(u - u_{fs})t_0 + h + u_{fs}t_0}{u} = t - t_0 - \frac{h}{u}.$$

Clearly

$$g'(u) = \frac{h}{u^2}$$

and

$$g(\hat{u}) = 0 \implies \hat{u} = \frac{h}{t - t_0} = u(t, t_0),$$

so

$$g'(\hat{u}) = \frac{(t - t_0)^2}{h},$$

and thus

$$\delta[t - t(u - u_{fs}, t_0)] = \frac{h}{(t - t_0)^2} \delta[u - u(t, t_0)].$$

Therefore we may also write

$$m_a(u, t) = f(u - u_{fs}) \frac{h}{(t - t_0)^2} \delta[u - u(t, t_0)]. \quad (4.17)$$

We are free to use either form for m_a , as a matter of convenience.

Step 2: Confirm m_a by testing mass conservation

The total ejected areal mass is

$$\int_0^\infty \int_0^\infty m_c(w, t_c) dw dt_c = \int_0^\infty f(w) dw \int_0^\infty \delta(t_c - t_0) dt_c = \int_0^\infty f(w) dw.$$

The total received areal mass is

$$\begin{aligned} \int_0^\infty \int_0^\infty m_a(u, t) du dt &= \int_0^\infty f(u - u_{fs}) du \int_0^\infty \delta[t - t(u - u_{fs}, t_0)] dt \\ &= \int_0^\infty f(u - u_{fs}) du \\ &= \int_{-u_{fs}}^\infty f(y) dy \\ &= \int_0^\infty f(y) dy \end{aligned}$$

where we used the substitution $y = u - u_{fs}$ and took advantage of the fact that the problem is defined so that all velocities are positive, i.e., $f(w) = 0$ for all $w < 0$.

This demonstrates that mass is conserved in this general case.

Step 3: Compute pressure at the surface and the pin

The pressure at the free surface is

$$P_c(t_c) = \int_0^\infty m_c(w, t_c) w dw = \delta(t_c - t_0) \int_0^\infty f(w) w dw.$$

The pressure at the sensor is

$$\begin{aligned}
P(t) &= \int_0^\infty m_a(u, t) u \, du = \int_0^\infty u f(u - u_{fs}) \frac{h}{(t - t_0)^2} \delta[u - u(t, t_0)] \, du \\
&= \frac{h}{(t - t_0)^2} u(t, t_0) f[u(t, t_0) - u_{fs}] \\
&= \frac{h^2}{(t - t_0)^3} f[u(t, t_0) - u_{fs}].
\end{aligned}$$

The recoil pressure is impulsive at the free surface, but extended over a finite interval at the sensor (unless f is also a delta function).

Step 4: Compare the true and inferred accumulated areal masses

The true accumulated areal mass is

$$\begin{aligned}
m_t(t) &= \int_0^t \int_0^\infty m_a(u, t') \, du \, dt' = \int_0^t \int_0^\infty f(u - u_{fs}) \frac{h}{(t - t_0)^2} \delta[u - u(t, t_0)] \, du \, dt' \\
&= \int_0^t \frac{h}{(t' - t_0)^2} f[u(t', t_0) - u_{fs}] \, dt'
\end{aligned}$$

and the inferred areal mass is

$$\begin{aligned}
m_i(t) &= \int_0^t \left(\frac{t' - t_0}{h} \right) P(t') \, dt' = \int_0^t \left(\frac{t' - t_0}{h} \right) \frac{h^2}{(t' - t_0)^3} f[u(t', t_0) - u_{fs}] \, dt' \\
&= \int_0^t \frac{h}{(t' - t_0)^2} f[u(t', t_0) - u_{fs}] \, dt'.
\end{aligned}$$

This confirms independently a finding from Section 3, namely that when ejecta production occurs instantaneously at the time of shock breakout, the inferred accumulated areal mass at the piezoelectric sensor will match the true (analytic) result (for a perfect system).

4.7 General case: Sustained constant production

The results from Sections 4.3 and 4.5, the latter in particular, reinforce the assertion that the piezoelectric analysis method exactly reproduces the correct result only when

the ejecta are produced instantaneously. We can investigate this for the general case of constant production and a separable velocity dependence by examining an areal mass function with form

$$m_c(w, t_c) = f(w) \prod_{t_0}^{t_1} (t_c) \quad (4.18)$$

This represents an areal mass function with sustained constant production where the velocity distribution of the ejecta does not evolve during the production window. Other models, such as those where the velocity distribution has a temporal dependence and is therefore not separable, are not represented by this function.

Step 1: Derive m_a

The areal mass function at the sensor is

$$\begin{aligned} m_a(u, t) &= \left(\frac{u}{u - u_{fs}} \right) m_c[u - u_{fs}, t_c(u - u_{fs}, t)] \\ &= \left(\frac{u}{u - u_{fs}} \right) f(u - u_{fs}) \prod_{t_0}^{t_1} \left[\frac{ut - (h + u_{fs}t_0)}{u - u_{fs}} \right] \\ &= \left(\frac{u}{u - u_{fs}} \right) f(u - u_{fs}) \prod_{t_0}^{t_1(u)} (t) \end{aligned}$$

where we have defined $t_0^a(u) \equiv t(u, t_0)$ and $t_1^a(u) \equiv t(u, t_1)$ and used the result from Section 4.3 to transform the boxcar from a function of creation time at the free surface to a function of arrival time at the sensor.

Step 2: Confirm m_a by testing mass conservation

The total ejected areal mass is

$$\int_0^\infty \int_0^\infty m_c(w, t_c) dw dt_c = (t_1 - t_0) \int_0^\infty f(w) dw$$

and the total received areal mass is

$$\begin{aligned} \int_0^\infty \int_0^\infty m_a(u, t) du dt &= \int_0^\infty \left(\frac{u}{u - u_{fs}} \right) f(u - u_{fs}) \int_0^{\infty t_1^a(u)} \prod_{t_0^a(u)} (t) dt du \\ &= \int_0^\infty \left(\frac{u}{u - u_{fs}} \right) f(u - u_{fs}) [t_1^a(u) - t_0^a(u)] du \\ &= \int_0^\infty \left(\frac{u}{u - u_{fs}} \right) f(u - u_{fs}) \left(\frac{u - u_{fs}}{u} \right) (t_1 - t_0) du \end{aligned}$$

$$\begin{aligned}
&= (t_1 - t_0) \int_0^\infty f(u - u_{fs}) \, du \\
&= (t_1 - t_0) \int_0^\infty f(y) \, dy
\end{aligned}$$

because, as above, $f(w) = 0$ for $w < 0$. This demonstrates that mass is conserved between the free surface and the sensor, indicating that our form for m_a is correct.

Step 3: Compute pressure at the surface and the pin

The pressure at the free surface is

$$P_c(t_c) = \int_0^\infty m_c(w, t_c) w \, dw = \prod_{t_0}^{t_1} (t_c) \int_0^\infty f(w) w \, dw$$

and the pressure at the piezo pin is

$$\begin{aligned}
P(t) &= \int_0^\infty m_a(u, t) u \, du = \int_0^\infty \left(\frac{u^2}{u - u_{fs}} \right) f(u - u_{fs}) \prod_{t_0}^{t_1(u)} (t) \, du \\
&= \int_{u(t_1, t)}^{u(t_0, t)} \left(\frac{u^2}{u - u_{fs}} \right) f(u - u_{fs}) \, du
\end{aligned}$$

where we have used

$$u(t_0, t') = \frac{h}{t' - t_0} \quad u(t_1, t') = \frac{h - u_{fs}(t_1 - t_0)}{t' - t_1}.$$

Step 4: Compare the true and inferred accumulated areal masses

The true accumulated areal mass is

$$m_t(t) = \int_0^t \int_0^\infty m_a(u, t) \, du \, dt = \int_0^t \int_{u(t_1, t')}^{u(t_0, t')} \left(\frac{u}{u - u_{fs}} \right) f(u - u_{fs}) \, du \, dt,$$

but the inferred accumulated areal mass is

$$m_i(t) = \int_0^t \left(\frac{t' - t_0}{h} \right) P(t') \, dt' = \int_0^t \int_{u(t_1, t')}^{u(t_0, t')} \left(\frac{t' - t_0}{h} \right) \left(\frac{u^2}{u - u_{fs}} \right) f(u - u_{fs}) \, du \, dt.$$

As expected, these expression differ.

4.8 General case: Arbitrary time dependence, single fixed velocity

The test problems in sections 4.3 and 4.5 were both chosen to deliberately violate the assumption of instantaneous ejecta creation. In TP2, the ejecta particles had a single velocity, but their production was constant over a finite interval. In TP4, there was again a single velocity, yet the production persisted indefinitely. In both cases, we found the final cumulative error in the inferred areal mass at the sensor was quite small, on the order of a few percent or even less, consistent with the general result derived in Section 3.

We might ask if this is will be true of any test problem where the production is not instantaneous but the ejecta are restricted to a single velocity. To that end, consider the areal mass function

$$m_c(w, t_c) = m_0 f(t_c) \delta(w - \bar{w}) \quad (4.19)$$

where $f(t_c)$ is any well-behaved function of time that could plausibly arise from the microphysics of ejecta production. Note the units on m_0 must be [mass · area⁻¹ · time⁻¹].

Step 1: Derive m_a

If, as usual, we define $\bar{u} \equiv \bar{w} + u_{fs}$, the areal mass function at the sensor becomes

$$m_a(u, t) = m_0 \left(\frac{u}{u - u_{fs}} \right) \delta(u - \bar{u}) f \left[\frac{ut - (h + u_{fs}t_0)}{u - u_{fs}} \right] \quad (4.20)$$

Step 2: Confirm m_a by testing mass conservation

The total ejected mass is

$$\int_0^\infty \int_0^\infty m_c(w, t_c) dw dt_c = \int_0^\infty \int_0^\infty m_0 f(t_c) \delta(w - \bar{w}) dw dt_c = m_0 \int_0^\infty f(t_c) dt_c.$$

The total received mass is given by

$$\int_0^\infty \int_0^\infty m_a(u, t) du dt = \int_0^\infty \int_0^\infty m_0 \left(\frac{u}{u - u_{fs}} \right) \delta(u - \bar{u}) f \left[\frac{ut - (h + u_{fs}t_0)}{u - u_{fs}} \right] du dt$$

$$= m_0 \left(\frac{\bar{u}}{\bar{u} - u_{fs}} \right) \int_0^\infty f \left[\frac{\bar{u}t - (h + u_{fs}t_0)}{\bar{u} - u_{fs}} \right] dt.$$

If we define the change of variables

$$y \equiv \frac{\bar{u}t - (h + u_{fs}t_0)}{\bar{u} - u_{fs}}$$

(note y is equivalent to a creation time at the free surface) this becomes

$$m_0 \left(\frac{\bar{u}}{\bar{u} - u_{fs}} \right) \int_{-\frac{h+u_{fs}t_0}{\bar{u}-u_{fs}}}^\infty f(y) \left(\frac{\bar{u} - u_{fs}}{\bar{u}} \right) dy = m_0 \int_0^\infty f(y) dy$$

because the problem is defined such that all times and velocities are positive. This demonstrates that mass is conserved and our expression for m_a is correct.

Step 3: Compute pressure at the surface and the pin

The pressure at the free surface is

$$P_c(t_c) = \int_0^\infty m_c(w, t_c) w dw = \int_0^\infty m_0 f(t_c) \delta(w - \bar{w}) w dw = m_0 \bar{w} f(t_c),$$

and the pressure on the sensor is

$$\begin{aligned} P(t) &= \int_0^\infty m_a(u, t) u du = \int_0^\infty m_0 \left(\frac{u^2}{u - u_{fs}} \right) \delta(u - \bar{u}) f \left[\frac{ut - (h + u_{fs}t_0)}{u - u_{fs}} \right] du \\ &= m_0 \left(\frac{\bar{u}^2}{\bar{u} - u_{fs}} \right) f \left[\frac{\bar{u}t - (h + u_{fs}t_0)}{\bar{u} - u_{fs}} \right]. \end{aligned}$$

Step 4: Compare the true and inferred accumulated areal masses

Let t_0^a denote the time of first arrival at the sensor. Then $t_0^a = t(\bar{w}, t_0) = t_0 + \frac{h}{\bar{u}}$.

The true accumulated areal mass at the sensor at an arrival time t is

$$\begin{aligned} m_t(t) &= \int_{t_0^a}^t \int_0^\infty m_a(u, t) du dt = m_0 \int_{t_0^a}^t \int_0^\infty \left(\frac{u}{u - u_{fs}} \right) \delta(u - \bar{u}) f \left[\frac{ut - (h + u_{fs}t_0)}{u - u_{fs}} \right] du dt \\ &= m_0 \int_{t_0^a}^t \left(\frac{\bar{u}}{\bar{u} - u_{fs}} \right) f \left[\frac{\bar{u}t - (h + u_{fs}t_0)}{\bar{u} - u_{fs}} \right] dt = m_0 \int_{y_0}^{y_1} f(y) dy \end{aligned}$$

where we have used the variable substitution from above, so

$$y_0 \equiv t_c(\bar{w}, t_0^a) \quad y_1 \equiv t_c(\bar{w}, t).$$

The inferred accumulated areal mass at the sensor is given by

$$\begin{aligned} m_i(t) &= \int_{t_0^a}^t \left(\frac{t' - t_0}{h} \right) P(t') dt' = \int_{t_0^a}^t \left(\frac{t' - t_0}{h} \right) m_0 \left(\frac{\bar{u}^2}{\bar{u} - u_{fs}} \right) f \left[\frac{\bar{u}t - (h + u_{fs}t_0)}{\bar{u} - u_{fs}} \right] dt' \\ &= \frac{m_0}{h} \left(\frac{\bar{u}^2}{\bar{u} - u_{fs}} \right) \int_{t_0^a}^t (t' - t_0) f \left[\frac{\bar{u}t - (h + u_{fs}t_0)}{\bar{u} - u_{fs}} \right] dt'. \end{aligned}$$

Let $t_0 = 0$ for simplicity, and again let us use our substitution variable, y . Then

$$\begin{aligned} m_i(t) &= \frac{m_0}{h} \left(\frac{\bar{u}^2}{\bar{u} - u_{fs}} \right) \int_{y_0}^{y_1} \frac{(\bar{u} - u_{fs})y + h}{\bar{u}} f(y) \left(\frac{\bar{u} - u_{fs}}{\bar{u}} \right) dy \\ &= \frac{m_0}{h} \int_{y_0}^{y_1} f(y) [(\bar{u} - u_{fs})y + h] dy \\ &= \frac{m_0}{h} (\bar{u} - u_{fs}) \int_{y_0}^{y_1} f(y)y dy + m_0 \int_{y_0}^{y_1} f(y) dy. \end{aligned}$$

Notice that the second term here is exactly the expression for the true areal mass. The mass inferred from the piezoelectric sensor data will always overestimate the true mass. This is to be expected, because when interpreting the data with the assumption of instantaneous creation, particles arriving later are assumed to have lower velocities, and thus must have higher masses to maintain the same level of momentum flux (pressure).

Thus, for the general case of an arbitrary time dependence and a single velocity, the time-dependent ratio of the inferred and true accumulated areal masses is

$$\frac{m_i(t)}{m_t(t)} \equiv \chi(t) = 1 + \left(\frac{\bar{w}}{h} \right) \frac{\int_0^{y_1} f(y)y dy}{\int_0^{y_1} f(y) dy} \quad (4.21)$$

where we have taken advantage of the fact that $y_0 = t_0 = 0$. (Recall y_1 contains the arrival time, t , because $y_1 = t_c(\bar{w}, t)$.) Note the similarity to the general result, Equation 3.1

The error percentage in the *total* accumulated mass is therefore

$$100 \left(\frac{\bar{w}}{h} \right) \frac{\int_0^{t_{cf}} f(y) y \, dy}{\int_0^{t_{cf}} f(y) \, dy} \quad (4.22)$$

where t_{cf} is the time at which ejecta production stops. For a typical setup [1], the fastest ejecta particles generally have $u_{ej} \approx 1.3 - 1.5 u_{fs}$. If $h = 18.57$ mm, $u_{fs} = 1.91$ mm/ μ s, and $\bar{w} = u_{ej} \approx 1.3 u_{fs}$ (such as for shot 6 of the above reference), we find $\frac{\bar{w}}{h} \approx 0.133 \mu\text{s}^{-1}$. If we say $\bar{w} = u_{ej} = 1.5 u_{fs}$ with $u_{fs} = 2.0$ mm/ μ s, and round h up to 20 mm, we find $\frac{\bar{w}}{h} = 0.15 \mu\text{s}^{-1}$. Other experiments [2, 3] situated the piezo pin at greater distances, such as 40 or 50 mm. So in general we expect $\frac{\bar{w}}{h} \approx 0.05 - 0.15 \mu\text{s}^{-1}$, with a typical value being $0.10 \mu\text{s}^{-1}$.

Consider the case of a sustained constant temporal dependence, namely

$$f(t_c) = \prod_{t_0=0}^{t_1} (t_c).$$

Equation 4.21 predicts the final ratio of inferred to true masses should be

$$1 + \frac{1}{2} \frac{\bar{w}}{h} t_1,$$

but recall that in Section 4.3 we derived the following expression for the mass ratio when $t > t_1^a$ and $t_0 = 0$:

$$\frac{\bar{u}}{h} \left[\frac{t_1^a + t_0^a}{2} \right].$$

It is straightforward to prove the equivalence of these expressions, because $t_1^a = t_0^a + \Delta t$, $t_0^a = \frac{h}{\bar{u}}$, and $\Delta t = \frac{\bar{w}}{\bar{u}} \Delta t_c = \frac{\bar{w}}{\bar{u}} t_1$.

The final error percentage in the total accumulated mass for TP2 is

$$100 \left(\frac{\bar{w}}{h} \right) \frac{\frac{1}{2} t_1^2}{t_1} = 50 \left(\frac{\bar{w}}{h} \right) t_1 \approx 5 t_1.$$

(Note the similarity between the second form, above, and the upper bound estimate in Equation 3.3.) If the ejecta production interval persists for 100 ns = 0.1 μ s, then the error in the total accumulated mass is 0.5%. The error rises to 5% if the ejecta production is allowed to persist for a full microsecond.

Consider the case

$$f(t_c) = \frac{2}{3} \frac{1}{t_c + \beta\tau}.$$

(Recall this gives an ejected areal mass akin to that predicted by the RMI source model.) Then the error at a given arrival time t is

$$100 \left(\frac{\bar{w}}{h} \right) \frac{\frac{2}{3} \left[y_1 - \beta\tau \ln \left(1 + \frac{y_1}{\beta\tau} \right) \right]}{\frac{2}{3} \ln \left(1 + \frac{y_1}{\beta\tau} \right)} = 100 \left(\frac{\bar{w}}{h} \right) \left[\frac{y_1}{\ln \left(1 + \frac{y_1}{\beta\tau} \right)} - \beta\tau \right].$$

Using typical values of $\frac{\bar{w}}{h} = 0.1 \text{ } \mu\text{s}^{-1}$, $\beta\tau = 10 \text{ ns}$, and $y_1 = 100 \text{ ns}$, this yields an error of 0.3%.

Using the same values for the case

$$f(y) = e^{-\frac{y}{y_0}}$$

produces an error of approximately 0.1%. Similarly, using

$$f(y) = e^{\frac{y}{y_0}}$$

gives an error of approximately 0.9% for the above values.

If the areal mass function at the source has a power-law dependence on time, i.e.,

$$f(y) = \left(\frac{y}{y_0} \right)^{-\alpha} \quad \alpha > 0, \alpha \neq 1, 2 \quad y_b < y < y_1$$

the error is given by

$$100 \left(\frac{\bar{w}}{h} \right) \left(\frac{\alpha - 1}{\alpha - 2} \right) \frac{y_1^{2-\alpha} - y_b^{2-\alpha}}{y_1^{1-\alpha} - y_b^{1-\alpha}}.$$

When $\alpha = 4$ and $y_b = 0.01 \text{ } \mu\text{s}$, while $y_1 = 0.1 \text{ } \mu\text{s}$ and $\frac{\bar{w}}{h} = 0.1 \text{ } \mu\text{s}^{-1}$ as above, the error is approximately 0.15%. When $\alpha = 2.1$ with the other parameters unchanged, the error rises to approximately 0.25%.

In general, $\chi \gg 1$ only when

$$\int_0^{t_{cf}} f(y) y \, dy \gg \int_0^{t_{cf}} f(y) \, dy$$

yet this is impossible for continuous nonnegative functions f when $0 < t_{cf} < 1$. (Because $y \cdot f(y) < f(y)$ when all $f \geq 0$ and all $y < 1$.) In the typical units for this problem (μs), t_{cf} will only exceed unity when the ejecta production interval exceeds a full microsecond.

4.9 General case: Arbitrary time dependence, arbitrary stationary velocity distribution

The previous section shows that piezoelectric sensor analysis can give a good measure of the ejecta areal mass even when the ejecta production has an arbitrary temporal dependence, as long as all ejecta have the same fixed velocity.

Now consider the most general case for an areal mass function with an arbitrary temporal dependence and a stationary velocity distribution:

$$m_c(w, t_c) = f(t_c)g(w). \quad (4.23)$$

Step 1: Derive m_a

Via Equation 2.14, the areal mass function at the sensor is simply

$$m_a(u, t) = \left(\frac{u}{u - u_{fs}} \right) f \left[\frac{ut - (h + u_{fs}t_0)}{u - u_{fs}} \right] g(u - u_{fs}). \quad (4.24)$$

Step 2: Confirm m_a by testing mass conservation

The total ejected mass is

$$\int_0^\infty f(t_c) dt_c \int_0^\infty g(w) dw.$$

The total received mass is

$$\int_0^\infty \int_0^\infty \left(\frac{u}{u - u_{fs}} \right) f \left[\frac{ut - (h + u_{fs}t_0)}{u - u_{fs}} \right] g(u - u_{fs}) dt du$$

which, after the substitution

$$y \equiv \frac{ut - (h + u_{fs}t_0)}{u - u_{fs}},$$

becomes (and now the order of integration is no longer arbitrary)

$$\int_0^\infty du \int_{-\frac{h+u_{fs}t_0}{u-u_{fs}}}^\infty g(u - u_{fs}) f(y) dy.$$

After applying the substitution $x \equiv u - u_{fs}$, this becomes

$$\int_{-u_{fs}}^\infty dx \int_{-\frac{h+u_{fs}t_0}{x}}^\infty g(x) f(y) dy = \int_0^\infty f(y) dy \int_0^\infty g(x) dx$$

because the problem is defined such that all times and velocities are positive. This verifies that mass is conserved.

Step 3: Compute pressure at the surface and the pin

The pressure on the free surface is given by

$$P_c(t_c) = \int_0^\infty m_c(w, t_c) w dw = f(t_c) \int_0^\infty g(w) w dw$$

and the pressure on the sensor is

$$P(t) = \int_0^\infty m_a(u, t) u du = \int_0^\infty \left(\frac{u^2}{u - u_{fs}} \right) f \left[\frac{ut - (h + u_{fs}t_0)}{u - u_{fs}} \right] g(u - u_{fs}) du.$$

Step 4: Compare the true and inferred accumulated areal masses

The true areal mass at the sensor is

$$\begin{aligned} m_t(t) &= \int_0^\infty du \int_{t_0^a}^t m_a(u, t') dt' \\ &= \int_0^\infty du \int_{t_0^a}^t \left(\frac{u}{u - u_{fs}} \right) f \left[\frac{ut' - (h + u_{fs}t_0)}{u - u_{fs}} \right] g(u - u_{fs}) dt' \\ &= \int_0^\infty du \int_{y_0}^{y_1} \left(\frac{u}{u - u_{fs}} \right) g(u - u_{fs}) f(y) \left(\frac{u - u_{fs}}{u} \right) dy \end{aligned}$$

$$= \int_0^\infty du g(u - u_{fs}) \int_{y_0}^{y_1} f(y) dy$$

where t_0^a is the time of first ejecta arrival at the sensor, $y_0 \equiv t_c(u, t_0^a) = t_0$, and $y_1 \equiv t_c(u, t)$.

For simplicity (but with no loss of generality) let us assume $t_0 = 0$. Then the inferred areal mass is given by

$$\begin{aligned} m_i(t) &= \int_{t_0^a}^t \left(\frac{t' - t_0}{h} \right) P(t') dt' \\ &= \int_{t_0^a}^t \frac{t'}{h} \int_0^\infty \left(\frac{u^2}{u - u_{fs}} \right) f \left[\frac{ut' - (h + u_{fs}t_0)}{u - u_{fs}} \right] g(u - u_{fs}) du \\ &= \frac{1}{h} \int_0^\infty du \int_{y_0}^{y_1} \frac{(u - u_{fs})y + h}{u} \left(\frac{u^2}{u - u_{fs}} \right) g(u - u_{fs}) f(y) \left(\frac{u - u_{fs}}{u} \right) dy \\ &= \frac{1}{h} \int_0^\infty du \int_{y_0}^{y_1} (u - u_{fs}) y g(u - u_{fs}) f(y) dy + \int_0^\infty g(u - u_{fs}) du \int_{y_0}^{y_1} f(y) dy. \end{aligned}$$

The second term is exactly the expression for the true accumulated areal mass. Therefore, the ratio of the inferred to true accumulated areal masses is

$$\begin{aligned} \frac{m_i(t)}{m_t(t)} &= \chi(t) = 1 + \frac{\int_0^\infty du (u - u_{fs}) g(u - u_{fs}) \int_0^{y_1} y f(y) dy}{h \int_0^\infty du g(u - u_{fs}) \int_0^{y_1} f(y) dy} \\ &= 1 + \frac{\int_0^\infty dw w g(w) \int_0^{y_1} y f(y) dy}{h \int_0^\infty dw g(w) \int_0^{y_1} f(y) dy} \end{aligned} \tag{4.25}$$

where again $y_1 = t_c(w, t)$. The units are consistent, because $w \cdot y$ has units of distance. Of course, this is a special case of the general result obtained in Section 3; note the similarity with Equation 3.1.

We can simplify further by considering the error in the *total* accumulated mass. This is the mass measured after all ejecta particles have been collected, which means the integral over creation times must span the entire creation interval. Let the final time of ejecta creation be t_{cf} . Then the error percentage in the total accumulated areal

mass is

$$\frac{100}{h} \frac{\int_0^\infty g(w) w \, dw \int_0^{t_{cf}} f(y) y \, dy}{\int_0^\infty g(w) \, dw \int_0^{t_{cf}} f(y) \, dy} = \frac{100}{h} \frac{G_1 F_1}{G_0 F_0} \quad (4.26)$$

where we have defined

$$G_n \equiv \int_0^\infty w^n g(w) \, dw = \int_0^{w_{ej}} w^n g(w) \, dw,$$

$$F_n \equiv \int_0^\infty y^n f(y) \, dy = \int_0^{t_{cf}} y^n f(y) \, dy.$$

and $w_{ej} = u_{ej} - u_{fs}$ represents the maximum ejecta velocity relative to the free surface. If, for example, $u_{ej} \approx 1.3u_{fs}$ as seen for several shots in [1], then $w_{ej} \approx 0.3u_{fs}$. For most cases, we expect $w_{ej} \lesssim 1$.

The error will become appreciable if (but not only if) $G_1 > G_0$ and $F_1 > F_0$. But previously, in Section 4.8, we found that for the typical limits of integration, no continuous nonnegative function f can satisfy $F_1 > F_0$. The same observation applies to g . In the typical units for this problem (mm, μs), *both upper limits of integration are less than unity* when the ejecta production does not persist for a full microsecond and the peak lab-frame ejecta velocity is less than twice the free surface velocity.

Consider sustained constant production of a flat velocity distribution:

$$f(t_c) = \prod_0^{t_1} (t_c) \quad \text{and} \quad g(w) = \prod_0^{w_{ej}} (w).$$

Then

$$\frac{F_1}{F_0} = \frac{t_1}{2}, \quad \frac{G_1}{G_0} = \frac{w_{ej}}{2}$$

and the error percentage becomes

$$25 \frac{w_{ej} t_1}{h}.$$

(Again, note the similarity to the upper bound estimate in Equation 3.3.) If the pin is located at a distance $h = 20$ mm, production persists for 100 ns = 0.1 μs , $u_{fs} = 1.91$ mm/ μs , and $u_{ej} = 2.0u_{fs} \implies w_{ej} = u_{fs}$, the error is $\approx 0.24\%$; the error rises to 2.4% if the production interval is 1 μs .

Cases where $G_1 > G_0$ may exist when w_{ej} significantly exceeds unity.

5 Analytic test problems with nonstationary velocity distributions

The examples in the preceding section established the validity of our formulation and demonstrated its application to stationary velocity distributions. We now turn our attention to the more general case of nonstationary velocity distributions.

5.1 TP5: RMI source model, single linearly increasing velocity

Let

$$m_c(w, t_c) = \frac{2}{3} \frac{m_0}{t_c + \beta\tau} \delta[w - \bar{w}(t_c)] \quad (5.1)$$

where

$$\bar{w}(t_c) = \begin{cases} w_0 + (w_1 - w_0) \frac{t_c}{t_c^*} & t_0 = 0 < t_c \leq t_c^* < t_1 = 1 \\ w_1 & t_0 = 0 < t_c^* < t_c < t_1 = 1 \end{cases} \quad (5.2)$$

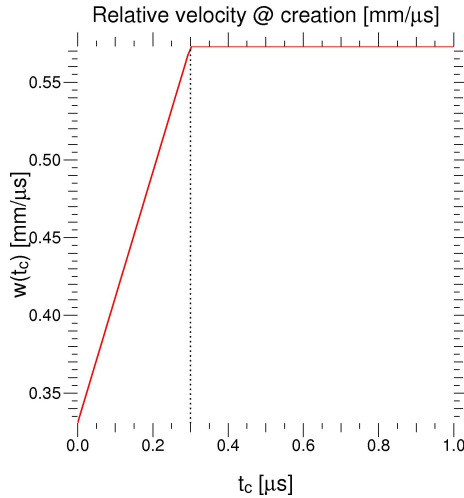


Figure 3: Time-dependent relative velocity, \bar{w} , plotted as a function of creation time, t_c . The situation depicted in this plot has $u_{fs} = 1.91 \text{ mm/}\mu\text{s}$, $u_1 = u_{ej} = 1.3u_{fs}$, $w_1 = u_1 - u_{fs} = 0.3u_{fs}$, and $w_0 = w_1/\sqrt{3}$. The values of u_{fs} and u_{ej} are taken from Shot 6 of [1]. As a thought experiment, the ejecta production persists for a full microsecond, and $t_c^* = 300 \mu\text{s}$. The dotted line marks t_c^* .

An example with $w_1 = \sqrt{3}w_0$ (motivated by the spike tip velocity in the RMI-based ejecta source model [4, 5, 6]), velocities taken from Shot 6 of [1], $t_c^* = 300$ ns, and a long (1 μ s) creation interval is plotted in Figure 3.

As we will see, this scenario gives rise to behaviors absent from our examinations of stationary velocity distributions. To aid the analysis, we also plot the ejecta arrival time as a function of creation time, and the lab-frame velocity of the arriving particles as a function of arrival time, in Figures 4 and 5. The initial distance to the pin, h , is 18.57 mm, per Shot 6 of [1], and the creation begins at $t_0 = 0$.

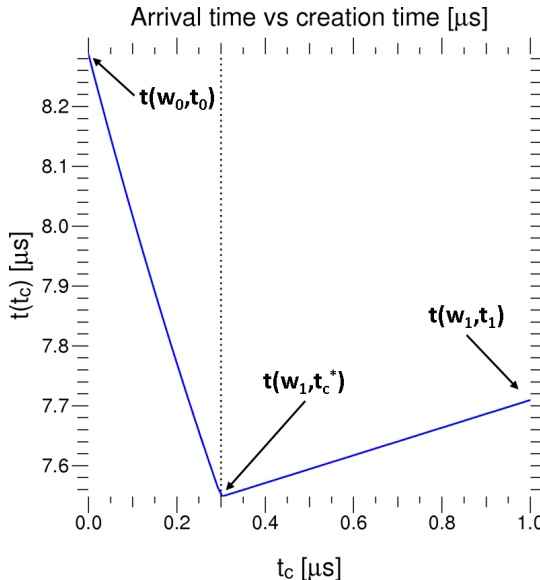


Figure 4: Arrival time, t , vs creation time, t_c . Note the earliest arrivals (lowest t values) are particles created at t_c^* (dotted line), and the latest arrivals are particles created at t_0 .

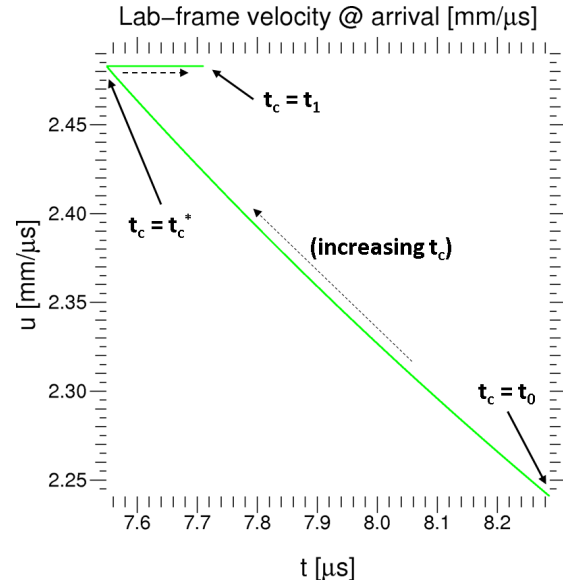


Figure 5: Lab-frame velocity vs arrival time. The horizontal portion of the plot is $u = u_1$. Note that for early arrival times, particles of 2 separate velocities arrive simultaneously.

These plots show that a simple linear velocity ramp can produce complicated behavior in the ejecta transit. For the specific parameters of this test problem, we find notable differences from our earlier test cases with stationary velocity distributions. In particular:

- There exists an arrival period during which ejecta particles created at two separate times (t_c) – or equivalently with two separate velocities (u) – arrive *simultaneously*.

- The earliest arrivals (lowest t values) are created neither at the beginning nor the end of the production interval, but at t_c^* . The first particles created are the last to arrive, meaning the ejecta cloud is partially “inverted” during transit.

Once the ejecta velocity attains its maximum value, w_1 , the kinematics are as we’d expect for the case of sustained production with a constant velocity (see test problems 2 and 4 in Sections 4.3 and 4.5). But prior to that, the slow-moving particles created early are overtaken by particles created later.

Step 1: Derive m_a

Before beginning, and so that we may periodically test our derivations, we note the units on m_0 must be [mass · area⁻¹]. Using $t_0 = 0$ in Equation 2.14, we have

$$m_a(u, t) = \left(\frac{u}{u - u_{fs}} \right) \frac{2}{3} \frac{m_0}{\frac{ut-h}{u-u_{fs}} + \beta\tau} \cdot \begin{cases} \delta \left[u - u_{fs} - \left(w_0 + \frac{w_1-w_0}{t_c^*} \frac{ut-h}{u-u_{fs}} \right) \right] & 0 < \frac{ut-h}{u-u_{fs}} \leq t_c^* \\ \delta(u - u_{fs} - w_1) & 0 < t_c^* < \frac{ut-h}{u-u_{fs}} \end{cases}$$

Let $u_0 \equiv w_0 + u_{fs}$ and $u_1 \equiv w_1 + u_{fs}$. Then $u_1 - u_0 = w_1 - w_0$ and

$$m_a(u, t) = \frac{2}{3} m_0 \frac{u}{ut - h + \beta\tau(u - u_{fs})} \cdot \begin{cases} \delta \left[u - u_0 - \frac{u_1 - u_0}{t_c^*} \frac{ut-h}{u-u_{fs}} \right] & 0 < \frac{ut-h}{u-u_{fs}} \leq t_c^* \\ \delta(u - u_1) & 0 < t_c^* < \frac{ut-h}{u-u_{fs}} \end{cases}$$

Now consider the inequalities defining the domain of validity of the two branches. We have

$$\frac{ut - h}{u - u_{fs}} \leq t_c^* \implies ut - h \leq (u - u_{fs})t_c^* \implies u(t - t_c^*) \leq h - u_{fs}t_c^*$$

but meanwhile, from Figure 4 we know the minimum arrival time is $t(w_1, t_c^*)$, so the minimum value of $t - t_c^*$ is given by

$$\frac{w_1 t_c^* + h}{u_1} - t_c^* = h - (u_1 - w_1)t_c^* = h - u_{fs}t_c^* \quad (5.3)$$

which is clearly positive because the definition of the problem clearly assumes the free surface has not arrived at the sensor by t_c^* . So $t - t_c^* > 0$ and

$$\frac{ut - h}{u - u_{fs}} \leq t_c^* \implies u \leq \frac{h - u_{fs}t_c^*}{t - t_c^*} = u(t_c^*, t),$$

meaning the areal mass function at the sensor can be written

$$m_a(u, t) = \frac{2}{3} m_0 \frac{u}{ut - h + \beta\tau(u - u_{fs})} \cdot \begin{cases} \delta\left[u - u_0 - \frac{u_1 - u_0}{t_c^*} \frac{ut - h}{u - u_{fs}}\right] & u \leq u(t_c^*, t) \\ \delta(u - u_1) & u > u(t_c^*, t) \end{cases}.$$

The argument of the delta function in the upper branch is a function of lab-frame velocity, u , for a given fixed arrival time, t . Let

$$f(u) \equiv u - u_0 - \left(\frac{u_1 - u_0}{t_c^*}\right) \frac{ut - h}{u - u_{fs}} \quad (5.4)$$

$$\implies f'(u) = 1 - \left(\frac{u_1 - u_0}{t_c^*}\right) \frac{h - u_{fs}t}{(u - u_{fs})^2}. \quad (5.5)$$

The roots of f are given by

$$\hat{u} - u_0 - \left(\frac{u_1 - u_0}{t_c^*}\right) \frac{\hat{u}t - h}{\hat{u} - u_{fs}} = 0 \implies \hat{u}^2 - (u_0 + u_{fs} + \alpha t)\hat{u} + (u_0 u_{fs} + \alpha h) = 0$$

where for simplicity we have defined $\alpha \equiv \frac{u_1 - u_0}{t_c^*}$. The roots of f are therefore

$$\hat{u}_{\pm}(t) \equiv \frac{u_0 + u_{fs} + \alpha t \pm \sqrt{(u_0 + u_{fs} + \alpha t)^2 - 4(u_0 u_{fs} + \alpha h)}}{2} \quad (5.6)$$

and, from Equation 4.1,

$$\delta[f(u)] = \frac{\delta[u - \hat{u}_+(t)]}{\left|1 - \left(\frac{u_1 - u_0}{t_c^*}\right) \frac{h - u_{fs}t}{[\hat{u}_+(t) - u_{fs}]^2}\right|} + \frac{\delta[u - \hat{u}_-(t)]}{\left|1 - \left(\frac{u_1 - u_0}{t_c^*}\right) \frac{h - u_{fs}t}{[\hat{u}_-(t) - u_{fs}]^2}\right|}.$$

We find that the quantity inside the absolute value brackets for the \hat{u}_+ term is always positive for the particular values examined here, likewise the quantity within the absolute value brackets for the \hat{u}_- term is always negative for these values, so

$$\delta[f(u)] = \frac{\delta[u - \hat{u}_+(t)]}{1 - \left(\frac{u_1 - u_0}{t_c^*}\right) \frac{h - u_{fs}t}{[\hat{u}_+(t) - u_{fs}]^2}} + \frac{\delta[u - \hat{u}_-(t)]}{\left(\frac{u_1 - u_0}{t_c^*}\right) \frac{h - u_{fs}t}{[\hat{u}_-(t) - u_{fs}]^2} - 1}. \quad (5.7)$$

Both zeroes of $f(u)$ are plotted together in Figure 6, and the lower value, $\hat{u}_-(t)$, is plotted by itself in Figure 7.

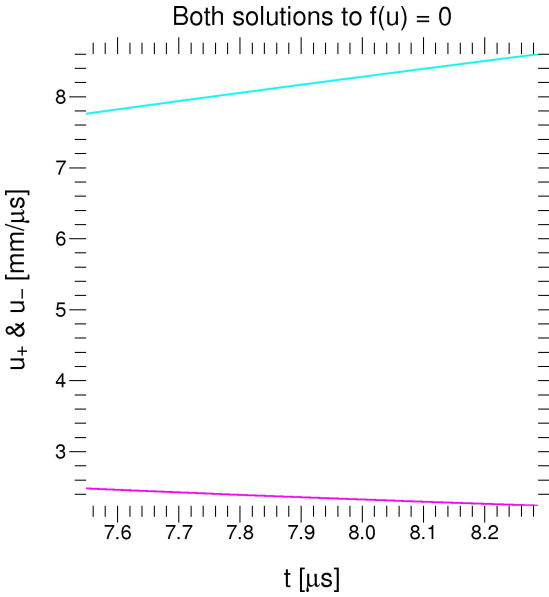


Figure 6: Roots of $f(u)$, $\hat{u}_+(t)$ and $\hat{u}_-(t)$, plotted as a function of ejecta arrival time, t . Note $\hat{u}_+ > u_1$ everywhere.

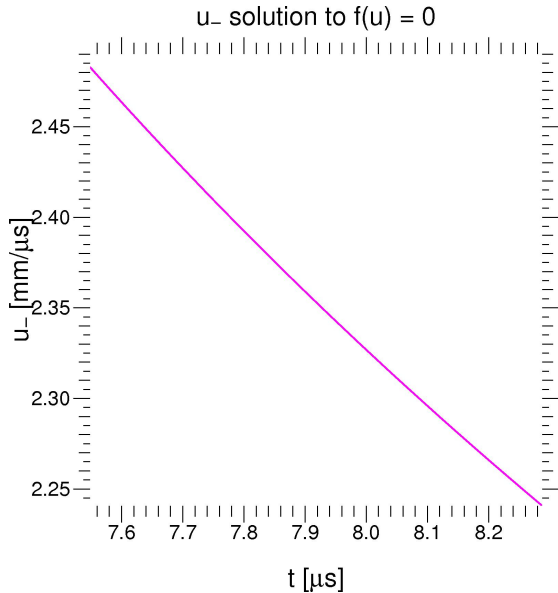


Figure 7: The lower root of $f(u)$, $\hat{u}_-(t)$, plotted as a function of ejecta arrival time, t . Compare Figure 5.

We see that $\hat{u}_+ > u_1$ at all times. Logically, however, all particles in the problem must have lab frame velocities $u_0 \leq u \leq u_1$. The \hat{u}_+ term in the delta function therefore cannot contribute to the solution. Meanwhile $\hat{u}_-(t)$ is exactly the portion of the plot in Figure 5 corresponding to ejecta particles emitted during $t_c \leq t_c^*$.

As a side note, we point out that when $\hat{u} \neq u_0$,

$$\begin{aligned} \hat{u} - u_0 - \left(\frac{u_1 - u_0}{t_c^*} \right) \frac{\hat{u}t - h}{\hat{u} - u_{fs}} = 0 &\implies - \left(\frac{u_1 - u_0}{t_c^*} \right) \frac{1}{\hat{u} - u_{fs}} = \frac{u_0 - \hat{u}}{\hat{u}t - h} \\ &\implies - \left(\frac{u_1 - u_0}{t_c^*} \right) \frac{h - u_{fs}t}{(\hat{u} - u_{fs})^2} = \frac{u_0 - \hat{u}}{\hat{u}t - h} \cdot \frac{h - u_{fs}t}{\hat{u} - u_{fs}} \end{aligned}$$

so

$$\left| 1 - \left(\frac{u_1 - u_0}{t_c^*} \right) \frac{h - u_{fs}t}{(\hat{u} - u_{fs})^2} \right| = \left| 1 + \frac{u_0 - \hat{u}}{\hat{u}t - h} \cdot \frac{h - u_{fs}t}{\hat{u} - u_{fs}} \right| = \left| 1 + \frac{\hat{u} - u_0}{\hat{u} - u_{fs}} \cdot \frac{h - u_{fs}t}{h - \hat{u}t} \right|.$$

When $\hat{u} = u_0$, we necessarily have $\hat{u}t = h \implies t = h/u_0 = t(w_0, t_0)$. The equivalence holds only when $\hat{u} \neq u_0$, but we know from Figure 7 that $u_0 \leq \hat{u}_-(t) \leq u_1$. For simplicity, then, it is better to keep $\delta[f(u)]$ in the form of Equation 5.7

Finally, then, and for completeness, the areal mass function at the sensor is

$$m_a(u, t) = \frac{2}{3} m_0 \frac{u}{ut - h + \beta\tau(u - u_{fs})} \cdot \begin{cases} \delta[f(u)] & u \leq u(t_c^*, t) \\ \delta(u - u_1) & u > u(t_c^*, t) \end{cases}. \quad (5.8)$$

where the full expression for $\delta[f(u)]$ is given by Equation 5.7, but we know *a priori* that the \hat{u}_+ term never contributes because $\hat{u}_+(t) > u_1 \geq u(t_c^*, t)$ for all times t .

Step 2: Confirm m_a by testing mass conservation

The total ejected mass over a period $t_0 < t_c < t_{cf} \leq t_1$ where $t_{cf} > t_c^*$ is

$$\begin{aligned} \int_0^{t_{cf}} \int_0^\infty m_c(w, t_c) dw dt_c &= \int_0^{t_c^*} \int_0^\infty m_c(w, t_c) dw dt_c + \int_{t_c^*}^{t_{cf}} \int_0^\infty m_c(w, t_c) dw dt_c = \\ &= \int_0^{t_c^*} \int_0^\infty \frac{2}{3} \frac{m_0}{t_c + \beta\tau} \delta \left[w - \left(w_0 + (w_1 - w_0) \frac{t_c}{t_c^*} \right) \right] dw dt_c + \int_{t_c^*}^{t_{cf}} \int_0^\infty \frac{2}{3} \frac{m_0}{t_c + \beta\tau} \delta(w - w_1) dw dt_c. \end{aligned}$$

Since $0 < w_0 \leq w \leq w_1 < \infty$, both delta functions are always satisfied within their respective domains of integration. The total ejected mass is therefore

$$\int_0^{t_{cf}} \frac{2}{3} \frac{m_0}{t_c + \beta\tau} dt_c = \frac{2}{3} m_0 \ln(t_c + \beta\tau) \Big|_0^{t_{cf}} = \frac{2}{3} m_0 \ln \left(1 + \frac{t_{cf}}{\beta\tau} \right).$$

In order to compute the total mass received by the sensor, we need to know the final arrival time when the creation interval extends to t_{cf} . From Figure 4, we know the arrival times must range from $t(w_1, t_c^*)$ to $\max[t(w_0, t_0), t(w_1, t_{cf})]$. Let us choose t_{cf} such that $t(w_1, t_{cf}) < t(w_0, t_0)$ as in Figure 4, where there $t_{cf} = t_1$. If the ejecta production interval persists sufficiently beyond $t_c = t_c^*$, it is possible to have scenarios where $t(w_1, t_{cf}) > t(w_0, t_0)$.

So, by fiat, the arrival times in this calculation cover the interval $t(w_1, t_c^*) \leq t \leq t(w_0, t_0)$.

The total received mass over the interval is therefore

$$\begin{aligned} \int_{t(w_1, t_c^*)}^{t(w_0, t_0)} \int_0^\infty m_a(u, t) du dt &= \int_{t(w_1, t_c^*)}^{t(w_0, t_0)} \int_0^{u(t_c^*, t)} m_a(u, t) du dt + \int_{t(w_1, t_c^*)}^{t(w_0, t_0)} \int_{u(t_c^*, t)}^\infty m_a(u, t) du dt \\ &\equiv I_1 + I_2 \end{aligned}$$

where

$$I_1 \equiv \int_{t(w_1, t_c^*)}^{t(w_0, t_0)} \int_0^{u(t_c^*, t)} \frac{2}{3} m_0 \frac{u}{ut - h + \beta\tau(u - u_{fs})} \cdot \frac{\delta[u - \hat{u}_-(t)]}{\left|1 - \left(\frac{u_1 - u_0}{t_c^*}\right) \frac{h - u_{fs}t}{[\hat{u}_-(t) - u_{fs}]^2}\right|} du dt$$

and

$$I_2 \equiv \int_{t(w_1, t_c^*)}^{t(w_1, t_{cf})} \int_{u(t_c^*, t)}^{\infty} \frac{2}{3} m_0 \frac{u}{ut - h + \beta\tau(u - u_{fs})} \delta(u - u_1) du dt$$

where we have used the observation, based on Figure 4, that the $u = u_1$ segment extends only from $t(w_1, t_c^*)$ to $t(w_1, t_{cf})$.

I₂:

We know, logically, that all lab-frame velocities in the problem cannot exceed u_1 . Thus $I_2 \neq 0$ requires $u(t_c^*, t) < u_1$ or

$$\frac{h - u_{fs}t_c^*}{t - t_c^*} < u_1 \implies t > \frac{(u_1 - u_{fs})t_c^* + h}{u_1} = t(w_1, t_c^*)$$

so the limits of integration over velocity, $[u(t_c^*, t), \infty] = [u(t_c^*, t), u_1]$ are distinct and encompass the root of the delta function as long as $t > t(w_1, t_c^*)$, which condition is exactly satisfied by the lower limit of the time integration. So the limits of integration on the double integral ensure the delta function will be nonzero for every t within the domain. Then

$$\begin{aligned} I_2 &= \int_{t(w_1, t_c^*)}^{t(w_1, t_{cf})} \frac{2}{3} m_0 \frac{u_1}{u_1 t - h + \beta\tau(u_1 - u_{fs})} dt = \frac{2}{3} m_0 \int_{t(w_1, t_c^*)}^{t(w_1, t_{cf})} \frac{dt}{t + \frac{(u_1 - u_{fs})\beta\tau - h}{u_1}} \\ &= \frac{2}{3} m_0 \ln \left[t + \frac{(u_1 - u_{fs})\beta\tau - h}{u_1} \right] \Big|_{t(w_1, t_c^*)=(w_1 t_{cf} + h)/u_1}^{t(w_1, t_{cf})=(w_1 t_{cf} + h)/u_1} \\ &= \frac{2}{3} m_0 \left\{ \ln \left[\frac{w_1 t_{cf} + h}{u_1} + \frac{(u_1 - u_{fs})\beta\tau - h}{u_1} \right] + \ln \left[\frac{w_1 t_c^* + h}{u_1} + \frac{(u_1 - u_{fs})\beta\tau - h}{u_1} \right] \right\} \\ &= \frac{2}{3} m_0 \ln \left(\frac{w_1 t_{cf} + w_1 \beta\tau}{w_1 t_c^* + w_1 \beta\tau} \right) = \frac{2}{3} m_0 \ln \left(\frac{t_{cf} + \beta\tau}{t_c^* + \beta\tau} \right). \end{aligned}$$

Because we defined $t_{cf} > t_c^*$, $I_2 > 0$.

I₁:

From the calculation of the total ejected mass, above, we know the correct final answer for the total received mass is

$$I_1 + I_2 = \frac{2}{3}m_0 \ln \left(1 + \frac{t_{cf}}{\beta\tau} \right).$$

Therefore, if our expression for I_1 is correct, and if we evaluate it correctly, we must find

$$I_1 = \frac{2}{3}m_0 \ln \left(\frac{t_{cf} + \beta\tau}{\beta\tau} \right) - \frac{2}{3}m_0 \ln \left(\frac{t_{cf} + \beta\tau}{t_c^* + \beta\tau} \right) = \frac{2}{3}m_0 \ln \left(1 + \frac{t_c^*}{\beta\tau} \right) \quad (5.9)$$

Although this seems surprising, perhaps even doubtful, numerical integrations confirm this, as shown below.

From Figure 7, we know $u_0 \leq \hat{u}_-(t) \leq u_1$, so the delta function in the velocity integration is guaranteed to contribute a nonzero value as long as $u(t_c^*, t) \leq u_1 \implies t \geq t(w_1, t_c^*)$, which is exactly the domain of integration. Thus

$$I_1 = \frac{2}{3}m_0 \int_{t(w_1, t_c^*)}^{t(w_0, t_0)} \frac{\hat{u}(t)}{\hat{u}(t)t - h + \beta\tau[\hat{u}(t) - u_{fs}]} \cdot \frac{dt}{\left| 1 - \left(\frac{u_1 - u_0}{t_c^*} \right) \frac{h - u_{fs}t}{[\hat{u}(t) - u_{fs}]^2} \right|}$$

where for simplicity we have denoted $\hat{u} \equiv \hat{u}_-$.

The analytic solution to I_1 is not immediately apparent, particularly given the expression for $\hat{u}_-(t)$ given in Equation 5.6. For now, we resort to testing this expression with numerical integrations.

Figure 8 shows the total ejected and received mass per unit area plotted as a function of t_{cf} for $t_c^* \leq t_{cf} \leq t_1$. In this calculation, we used the same parameters used to derive the plots in Figures 3 - 5, namely $u_{fs} = 1.91 \text{ mm}/\mu\text{s}$, $u_1 = u_{ej} = 1.3u_{fs}$, $w_0 = w_1/\sqrt{3}$, $h = 18.57 \text{ mm}$, and $t_c^* = 0.3 \mu\text{s}$. Furthermore, we set $m_0 = 0.01 \text{ mg}/\text{mm}^2$ and $\beta\tau = 10.2 \text{ ns}$ (motivated by FLAG calculations of Shot 6 of [1].) When the numerical integrations are performed on a time mesh with $\Delta t_c = 10^{-5} \mu\text{s}$, the calculated total received mass overestimates the analytically computed total ejected mass by between 0.010% and 0.013%. The error continues to decrease with decreasing Δt_c . This establishes that mass is conserved, meaning our expressions for $m_a(u, t)$ and its double integration are correct. The math has been performed correctly.

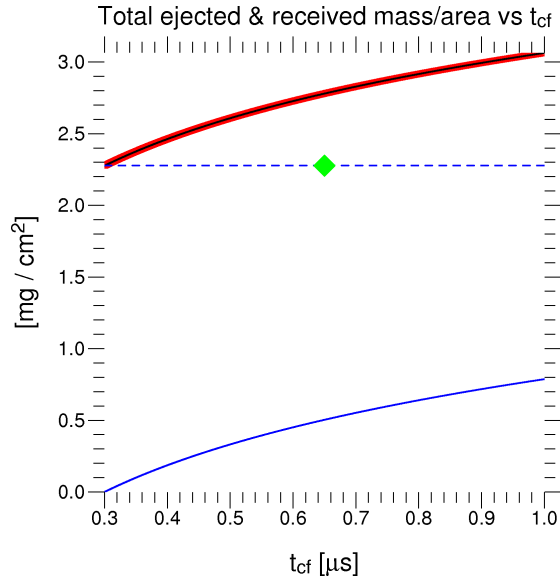


Figure 8: Total mass ejected over the interval $[t_0, t_{cf}]$ ($t_{cf} > t_c^*$) and received over the equivalent interval at the sensor. The analytic solution for the total ejected mass (black) is plotted against the total received mass (red). The width of the red line is *not* an error bar; the symbol size was magnified to make the red and black lines simultaneously visible, otherwise they would overlap each other. The total received mass was computed as the sum of I_2 (solid blue), which was computed analytically, and I_1 (dashed blue), which was computed numerically. The green diamond represents the analytically computed value of $\frac{2}{3}m_0 \ln(1 + \frac{t_c^*}{\beta\tau})$, which proves Equation 5.9 is correct.

Step 3: Compute pressure at the surface and the pin

We can now compute the total pressure on the free surface and on the sensor.

The pressure on the free surface is

$$\begin{aligned}
 P_c(t_c) &= \int_0^\infty m_c(w, t_c) w \, dw = \int_0^\infty \frac{2}{3}m_0 \frac{w}{t_c + \beta\tau} \delta[w - \bar{w}(t_c)] \, dw \\
 &= \frac{2}{3} \frac{m_0}{t_c + \beta\tau} \cdot \begin{cases} w_0 + \frac{(w_1 - w_0)t_c}{t_c^*} & 0 < t_c \leq t_c^* < t_1 \\ w_1 & 0 < t_c^* < t_c \leq t_1 \end{cases}.
 \end{aligned}$$

The units work. As expected, this is a smooth function of t_c , although the unphysically discontinuous nature of $\bar{w}'(t_c)$ puts a tiny kink at $P(t_c^*)$. The free surface pressure is plotted below in Figure 9.

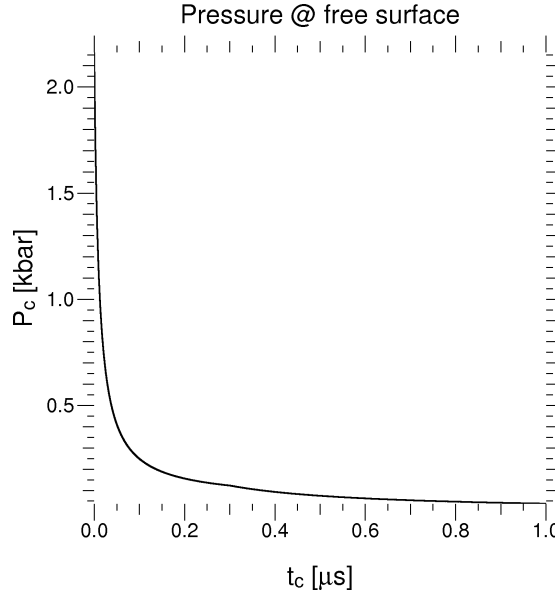


Figure 9: Pressure on the free surface, computed analytically.

The pressure on the sensor is given by

$$\begin{aligned}
P(t) &= \int_0^\infty m_a(u, t) u \, du = \int_0^{u(t_c^*, t)} m_a(u, t) u \, du + \int_{u(t_c^*, t)}^\infty m_a(u, t) u \, du \\
&= \int_0^{u(t_c^*, t)} \frac{2}{3} m_0 \frac{u^2}{ut - h + \beta \tau(u - u_{fs})} \cdot \frac{\delta[u - \hat{u}_-(t)]}{\left| 1 - \left(\frac{u_1 - u_0}{t_c^*} \right) \frac{h - u_{fs}t}{[\hat{u}_-(t) - u_{fs}]^2} \right|} \, du \\
&\quad + \int_{u(t_c^*, t)}^\infty \frac{2}{3} m_0 \frac{u^2}{ut - h + \beta \tau(u - u_{fs})} \delta(u - u_1) \, du \\
&\equiv P_1 + P_2.
\end{aligned}$$

The delta function in P_1 gives a nonzero contribution as long as $u(t_c^*, t) = \frac{h - u_{fs}t_c^*}{t - t_c^*} > \hat{u}_-(t)$. Numerical comparisons find this is always satisfied for $t < t(w_0, t_0)$, which is the final arrival time. Similarly, the delta function in P_2 gives a nonzero contribution as long as $u(t_c^*, t) < u_1$, or $t > t(w_1, t_c^*)$, which is the earliest arrival time. So the

sifting property applies to both integrals. Thus

$$P_1(t) = \begin{cases} 0 & t < t(w_1, t_c^*) \\ \frac{2}{3} m_0 \frac{\hat{u}(t)^2}{\hat{u}(t)t - h + \beta\tau(\hat{u} - u_{fs})} \frac{1}{\left| 1 - \left(\frac{u_1 - u_0}{t_c^*} \right) \frac{h - u_{fs}t}{[\hat{u}y(t) - u_{fs}]^2} \right|} & t(w_1, t_c^*) < t < t(w_0, t_0) \\ 0 & t > t(w_0, t_0) \end{cases}$$

(where again for brevity $\hat{u} = \hat{u}_-$), and

$$P_2(t) = \begin{cases} 0 & t < t(w_1, t_c^*) \\ \frac{2}{3} m_0 \frac{u_1^2}{u_1 t - h + \beta\tau(u_1 - u_{fs})} & t(w_1, t_c^*) < t < t(w_1, t_1) \\ 0 & t(w_1, t_1) < t \end{cases}$$

The result is plotted in Figures 10 and 11. Note that the pressure must drop to 0 after the final ejecta hit the sensor, which in this example is $\sim 1.5 \mu\text{s}$ prior to the arrival of the free surface.

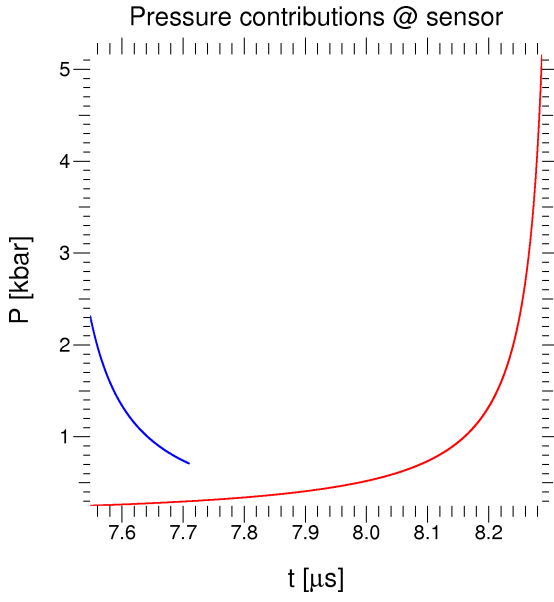


Figure 10: Contributions to the pressure at the sensor. P_2 (blue) was computed analytically; P_1 (red) was computed numerically. The free surface arrives at the sensor at $t_{fs} = 9.72 \mu\text{s}$.

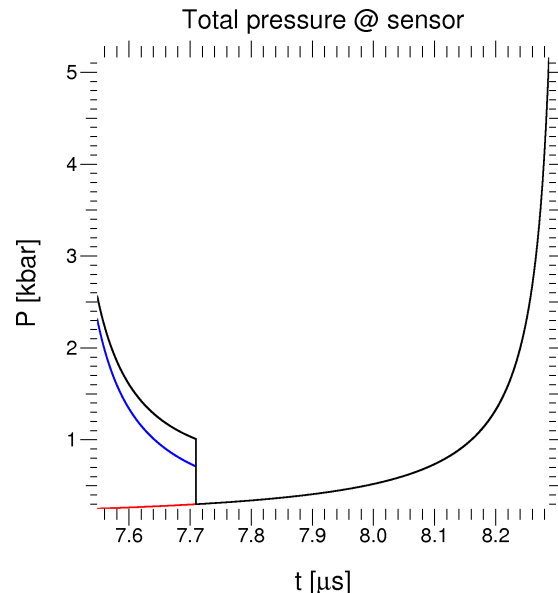


Figure 11: Total pressure at the sensor (black) computed from the sum of P_2 (blue, analytic) and P_1 (red, numerical). The free surface arrives at the sensor at $t_{fs} = 9.72 \mu\text{s}$.

The pressure on the sensor is discontinuous at $t(w_1, t_1)$. Prior to this time, the pressure has contributions from ejecta with two different velocities arriving simultaneously. The particles launched after t_c^* have a constant velocity ($u = u_1$) as a function of creation time, but the incremental mass per unit time is decreasing, so the momentum flux from those particles is *declining*. The particles launched prior to t_c^* also encapsulate the diminishing mass per unit creation time, but this portion of the ejecta cloud is inverted before it arrives at the sensor, meaning the sensor sees ejecta with an increasing mass per unit creation time. Thus the momentum flux of particles created prior to t_c^* *increases* with time. The discontinuity arises from the arbitrary creation cutoff time, t_1 , which causes one contribution to the pressure to vanish instantaneously. If the creation interval were sufficiently long, the declining pressure from the faster $t_c > t_c^*$ particles would eventually match the rising pressure from the slower $t_c < t_c^*$ particles, and the pressure on the sensor would no longer be discontinuous.

The voltage generated at the piezoelectric sensor is proportional to $\frac{dP}{dt}$, as explained in Appendix A. The voltage calculated from the pressure on the sensor is plotted in Figure 12.

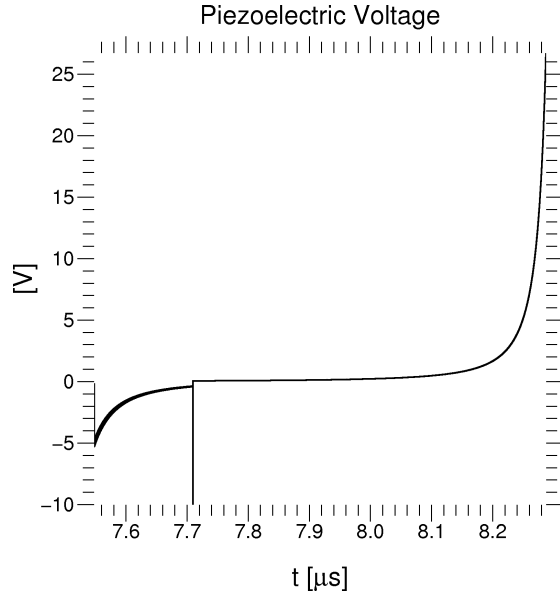


Figure 12: Piezoelectric voltage computed from the pressure at the sensor. The large negative excursion at $t = t(w_1, t_1)$ is an artifact of numerical differentiation over a discontinuity. In this scenario, the free surface arrives at the sensor at $t_{fs} = 9.72 \mu s$, almost $1.5 \mu s$ after the last ejecta particles have arrived.

Step 4: Compare the true and inferred accumulated areal masses

Finally, we are in a position to compare the true and inferred accumulated areal masses at the sensor.

The *true* accumulated areal mass at the sensor for $t(w_1, t_c^*) \leq t \leq t(w_0, t_0)$ is

$$m_t(t) = \int_0^t \int_0^\infty m_a(u, t') du dt' = \int_{t(w_1, t_c^*)}^t dt' \int_0^{u(t_c^*, t')} m_a(u, t') du + \int_{t(w_1, t_c^*)}^t dt' \int_{u(t_c^*, t')}^\infty m_a(u, t') du \\ \equiv M_1 + M_2$$

where

$$M_1 = \int_{t(w_1, t_c^*)}^t dt' \int_0^{u(t_c^*, t')} \frac{2}{3} m_0 \frac{u}{ut - h + \beta\tau(u - u_{fs})} \cdot \frac{\delta[u - \hat{u}_-(t')]}{\left|1 - \left(\frac{u_1 - u_0}{t_c^*}\right) \frac{h - u_{fs}t'}{[\hat{u}_-(t') - u_{fs}]^2}\right|} du$$

and

$$M_2 = \int_{t(w_1, t_c^*)}^t dt' \int_{u(t_c^*, t')}^\infty \frac{2}{3} m_0 \frac{u}{ut - h + \beta\tau(u - u_{fs})} \delta(u - u_1) du.$$

M_1 represents the contribution from ejecta created prior to t_c^* (i.e., ejecta created while the relative velocity of creation varies), and M_2 represents the contribution from ejecta created after t_c^* (i.e., ejecta created while the relative velocity of creation is constant). Thus M_2 reaches its maximum value when $t = t(w_1, t_1)$ after which it is constant (because all of the constant-velocity ejecta have already arrived and can no longer contribute to the areal mass, as shown in Figures 4 and 5). M_1 reaches its maximum value when $t = t(w_0, t_0)$, which is the time at which the final ejecta particles arrive; after this time, no new ejecta arrive at the sensor.

Because the integrations are very similar, our careful work examining the calculations for mass conservation (Step 2) are a useful guide.

As before, the second integral can be computed analytically. We find

$$M_2 = \frac{2}{3} m_0 \int_{t(w_1, t_c^*)}^t \frac{dt'}{t' + \frac{(u_1 - u_{fs})\beta\tau - h}{u_1}} = \frac{2}{3} m_0 \ln \left[t' + \frac{(u_1 - u_{fs})\beta\tau - h}{u_1} \right]_{t(w_1, t_c^*)}^t \\ = \frac{2}{3} m_0 \left\{ \ln \left[\frac{u_1 t + (u_1 - u_{fs})\beta\tau - h}{u_1} \right] - \ln \left[\frac{w_1 t_c^* + h + (u_1 - u_{fs})\beta\tau - h}{u_1} \right] \right\}$$

$$= \frac{2}{3} m_0 \ln \left[\frac{\left(\frac{u_1}{w_1} \right) t + \beta \tau - \left(\frac{h}{w_1} \right)}{t_c^* + \beta \tau} \right]$$

for $t < t(w_1, t_1) = \frac{w_1 t_1 + h}{u_1}$ and

$$M_2 = \frac{2}{3} m_0 \ln \left[\frac{t_1 + \beta \tau}{t_c^* + \beta \tau} \right]$$

for $t \geq t(w_1, t_1)$. In the latter case, note $M_2 = I_2$ from the mass-conservation calculations in Step 2, when $t_{cf} = t_1$.

As with the mass-conservation calculation we compute the first term, M_1 , using numerical integrations. As a sanity check, we know from the mass conservation tests in Step 2 that when $t = t(w_0, t_0)$, we must find

$$M_1 = \frac{2}{3} m_0 \ln \left(1 + \frac{t_c^*}{\beta \tau} \right).$$

This is exactly what we obtain from the numerical integrations.

The *inferred* accumulated areal mass at the sensor is given by

$$m_i(t) = \int_{t(w_1, t_c^*)}^t \left(\frac{t' - t_0}{h} \right) P(t') dt' = \frac{1}{h} \int_{t(w_1, t_c^*)}^t t' P(t') dt'$$

where $P(t)$ is the function plotted in black in Figure 11 (see above for the calculation of that curve). We compute this function through numerical integrations.

The results for the true and inferred areal masses are plotted in Figure 13.

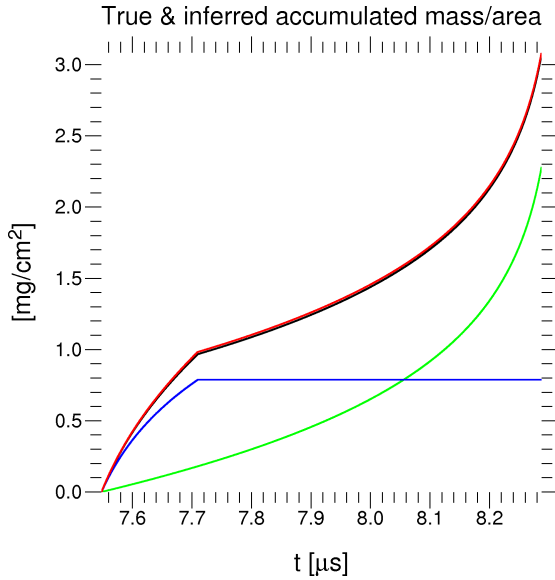


Figure 13: True and inferred mass/area at the sensor *as a function of arrival time*. Blue: M_2 , computed analytically. Green: M_1 , computed numerically. Black: True accumulated areal mass ($M_1 + M_2$). Red: Inferred accumulated areal mass derived from the pressure at the sensor. Note the excellent agreement between the true and inferred values. This calculation used $u_{fs} = 1.91$ mm/μs, $u_1 = u_{ej} = 1.3u_{fs}$, $w_1 = u_1 - u_{fs} = 0.3u_{fs}$, $w_0 = w_1/\sqrt{3}$, $t_0 = 0$, $t_1 = 1$ μs, $t_c^* = 0.3$ μs, $m_0 = 0.01$ mg/mm², and $\beta\tau = 10.2$ ns.

We note the final value of the true mass at $t(w_0, t_0)$ agrees with that computed for the total ejected and total received masses at $t_{cf} = t_1$ in Figure 8. This is a useful sanity check, and lends confidence in these numerical integrations.

We find the true and inferred areal masses agree extremely well. Outside the first nanosecond, where numerical errors dominate, the inferred value overestimates the true value by less than 2%.

This reaffirms the results derived in Section 3. This test problem was designed to strain the piezoelectric sensor analysis technique. Nevertheless, we find that for this problem – which is motivated by the RMI ejecta source model [4, 5, 6], with physical parameters taken from the published results from Shot 6 of [1] – the mass/area of the ejecta cloud that would be inferred from a perfect piezoelectric measurement is a very close match to the true analytic result.

5.2 General case: Arbitrary time dependence, single linearly increasing velocity

We note that in TP5, the behavior of $m_c(w, t_c)$ for $t_c > t_c^*$ is effectively that examined in TP4 (with $t_0 = t_c^*$). From that analysis we know the error in the inferred accumulated areal mass at the sensor will be small for that contribution. Thus, in this section we confine our examination to times $t_c < t_c^*$, or more generally, we consider the case where the relative velocity w varies linearly across the creation interval of interest.

Furthermore, we are motivated by the observation that the functional form of $\bar{w}(t_c)$ in TP5 almost makes m_c a function of t_c only.

When $t_c < t_c^*$, the areal mass function at the source in TP5 can be written

$$m_c(w, t_c) = \frac{2}{3} \frac{m_0}{t_c + \beta\tau} \delta(w - w_0 - \alpha t_c) \equiv \frac{2}{3} \frac{m_0}{t_c + \beta\tau} \delta[j(t_c)]$$

where we have again defined $\alpha \equiv \frac{w_1 - w_0}{t_c^*}$. Then $j'(t_c) = -\alpha$ and

$$j(\hat{t}_c) = 0 \implies \hat{t}_c = \frac{w - w_0}{\alpha} \equiv \hat{t}_c(w)$$

so

$$m_c(w, t_c) = \frac{2}{3} \frac{m_0}{t_c + \beta\tau} \frac{1}{\alpha} \delta[t_c - \hat{t}_c(w)].$$

Therefore, let us consider the general case of an arbitrary temporal dependence and a single linearly increasing relative velocity at creation:

$$m_c(w, t_c) = f(t_c) \delta[t_c - \hat{t}_c(w)] \quad (5.10)$$

where $\hat{t}_c(w)$ is given above (i.e., the relative velocity at creation increases linearly from w_0 at $t_c = t_0 = 0$ to w_1 at $t_c = t_c^*$.)

Step 1: Derive m_a

From Equation 2.14, we have

$$m_a(u, t) = \left(\frac{u}{u - u_{fs}} \right) f \left(\frac{ut - h}{u - u_{fs}} \right) \delta \left[\frac{ut - h}{u - u_{fs}} - \hat{t}_c(u - u_{fs}) \right].$$

Now,

$$\hat{t}_c(u - u_{fs}) = \frac{u - u_{fs} - w_0}{\alpha} \equiv \frac{u - u_0}{\alpha}$$

where as usual we have defined $u_0 = w_0 + u_{fs}$. If we define

$$g(t) \equiv \frac{ut - h}{u - u_{fs}} - \frac{u - u_0}{\alpha},$$

then

$$\delta[g(t)] = \left(\frac{u - u_{fs}}{u} \right) \delta[t - \hat{t}(u)]$$

where

$$\hat{t}(u) = \frac{h}{u} + \frac{u - u_0}{u_1 - u_0} \frac{u - u_{fs}}{u} t_c^*.$$

Then the areal mass function at the sensor becomes

$$m_a(u, t) = f \left(\frac{ut - h}{u - u_{fs}} \right) \delta[t - \hat{t}(u)]. \quad (5.11)$$

Step 2: Confirm m_a by testing mass conservation

The total ejected mass is

$$\int_0^\infty dw \int_{t_0}^{t_c^*} m_c(w, t_c) dt_c = \int_{w_0}^{w_1} dw \int_0^{t_c^*} f(t_c) \delta[t_c - \hat{t}_c(w)] dt_c$$

Inside the t_c integral, w is fixed and $0 < \hat{t}_c(w) < t_c^*$, so the sifting property always applies. The above expression becomes

$$\int_{w_0}^{w_1} f[\hat{t}_c(w)] dw = \int_{w_0}^{w_1} f\left(\frac{w - w_0}{\alpha}\right) dw.$$

Let $x \equiv \frac{w - w_0}{\alpha}$. Then the expression for the total ejected mass becomes

$$\alpha \int_0^{t_c^*} f(x) dx.$$

The total received mass is

$$\int_0^\infty du \int_0^\infty m_a(u, t) dt = \int_{u_0}^{u_1} du \int_0^\infty f\left(\frac{ut - h}{u - u_{fs}}\right) \delta[t - \hat{t}(u)] dt.$$

Within the t integral, u is fixed and

$$\frac{h}{u_0} < \hat{t}(u) < \frac{h}{u_1} + \left(\frac{u_1 - u_{fs}}{u_1} \right) t_c^*$$

so the sifting property applies across the domain of integration, and the expression becomes

$$\int_{u_0}^{u_1} f \left[\frac{u\hat{t}(u) - h}{u - u_{fs}} \right] du.$$

Now,

$$\frac{u\hat{t}(u) - h}{u - u_{fs}} = \left(\frac{u - u_0}{u_1 - u_0} \right) t_c^* = \frac{u - u_0}{\alpha}$$

where we have used the fact that $w_1 - w_0 = u_1 - u_0$. Thus the total received mass is

$$\int_{u_0}^{u_1} f \left(\frac{u - u_0}{\alpha} \right) du.$$

Let $z \equiv \frac{u - u_0}{\alpha}$. Then the expression for the total received mass becomes

$$\alpha \int_0^{t_c^*} f(z) dz,$$

which is exactly equivalent to the above expression for the total ejected mass. This verifies that mass is conserved and our expression for m_a is valid.

Step 3: Compute pressure at the surface and the pin

(This is irrelevant for our current purposes. See below.)

Step 4: Compare the true and inferred accumulated areal masses

The general expression for the true accumulated areal mass at the sensor is

$$m_t(t) = \int_0^t \int_0^\infty m_a(u, t') du dt'$$

and the general expression for the inferred accumulated areal mass at the sensor is

$$m_i(t) = \int_0^t \left(\frac{t' - t_0}{h} \right) P(t') dt' = \int_0^t \left(\frac{t' - t_0}{h} \right) \left[\int_0^\infty m_a(u, t') u du \right] dt'$$

$$= \frac{1}{h} \int_0^t \int_0^\infty m_a(u, t') u t' du dt'$$

where as usual we have set $t_0 = 0$ for convenience.

Because our expression for m_a contains a delta function on t , it is highly convenient to swap the order of integrations in these expressions. Then the expression for the true accumulated areal mass becomes

$$\begin{aligned} m_t(t) &= \int_0^\infty \int_0^t m_a(u, t') dt' du = \int_0^\infty \int_0^t \left(\frac{u}{u - u_{fs}} \right) f \left[\frac{ut' - h}{u - u_{fs}} \right] \delta[g(t')] dt' du \\ &= \int_0^\infty \int_0^t \left(\frac{u}{u - u_{fs}} \right) f \left[\frac{ut' - h}{u - u_{fs}} \right] \left(\frac{u - u_{fs}}{u} \right) \delta[t' - \hat{t}(u)] dt' du \\ &= \int_{u_0}^{u_1} du \int_0^t f \left[\frac{ut' - h}{u - u_{fs}} \right] \delta[t' - \hat{t}(u)] dt'. \end{aligned}$$

The delta function will have a nonzero contribution (i.e., the sifting property will apply) when $0 < \hat{t}(u) < t$ or

$$0 < \frac{h}{u} + \frac{(u - u_0)(u - u_{fs})}{u\alpha} < t \implies \frac{(u - u_0)(u - u_{fs})}{\alpha} < ut - h$$

or

$$u < \hat{u}_\pm(t)$$

where \hat{u}_\pm are the expressions in Equation 5.6. From our previous explorations we know $\hat{u}_+(t) > u_1$ for all arrival times t , so that solution always exceeds the largest velocities in the problem. Therefore the sifting property applies only for $u < \hat{u}_-(t)$, and the true accumulated areal mass can be written

$$m_t(t) = \int_{u_0}^{\hat{u}_-(t)} du \int_0^t f \left[\frac{ut' - h}{u - u_{fs}} \right] \delta[t' - \hat{t}(u)] dt' = \int_{u_0}^{\hat{u}_-(t)} f \left[\frac{u\hat{t}(u) - h}{u - u_{fs}} \right] du.$$

Now

$$\begin{aligned} \frac{u\hat{t}(u) - h}{u - u_{fs}} &= \frac{1}{u - u_{fs}} \left[u \left(\frac{h}{u} + \frac{(u - u_0)(u - u_{fs})}{u\alpha} \right) - h \right] = \frac{1}{u - u_{fs}} \left[\frac{(u - u_0)(u - u_{fs})}{\alpha} \right] \\ &= \frac{u - u_0}{\alpha}, \end{aligned}$$

so

$$m_t(t) = \int_{u_0}^{\hat{u}_-(t)} f \left(\frac{u - u_0}{\alpha} \right) du.$$

Using the variable substitution $y \equiv \frac{u-u_0}{\alpha}$, the expression for the true accumulated areal mass becomes, finally,

$$m(t) = \alpha \int_0^{y_1(t)} f(y) dy$$

where we have defined $y_1(t) \equiv \frac{\hat{u}_-(t)-u_0}{\alpha}$.

Similarly, the expression for the inferred accumulated areal mass becomes

$$\begin{aligned} m(t) &= \frac{1}{h} \int_{u_0}^{u_1} du \int_0^t f\left[\frac{ut' - h}{u - u_{fs}}\right] \delta[t' - \hat{t}(u)] u t' dt' \\ &= \frac{1}{h} \int_{u_0}^{\hat{u}_-(t)} f\left(\frac{u - u_0}{\alpha}\right) u \left[\frac{h}{u} + \frac{(u - u_0)(u - u_{fs})}{u\alpha}\right] du \\ &= \int_{u_0}^{\hat{u}_-(t)} f\left(\frac{u - u_0}{\alpha}\right) du + \frac{1}{h\alpha} \int_{u_0}^{\hat{u}_-(t)} f\left(\frac{u - u_0}{\alpha}\right) (u - u_0) (u - u_{fs}) du, \end{aligned}$$

and after again using the substitution $y \equiv \frac{u-u_0}{\alpha}$, as above, the inferred accumulated areal mass becomes

$$\begin{aligned} m(t) &= \alpha \int_0^{y_1(t)} f(y) dy + \frac{1}{h} \int_0^{y_1(t)} f(y) y (\alpha y + u_0 - u_{fs}) \alpha dy \\ &= \alpha \int_0^{y_1(t)} f(y) dy + \frac{\alpha w_0}{h} \int_0^{y_1(t)} y f(y) dy + \frac{\alpha^2}{h} \int_0^{y_1(t)} y^2 f(y) dy \end{aligned}$$

where we have used $w_0 = u_0 - u_{fs}$.

The ratio of the inferred and true accumulated areal masses is therefore

$$\frac{m_i(t)}{m_t(t)} = \chi(t) = 1 + \frac{w_0}{h} \cdot \frac{\int_0^{y_1(t)} y f(y) dy}{\int_0^{y_1(t)} f(y) dy} + \frac{\alpha}{h} \cdot \frac{\int_0^{y_1(t)} y^2 f(y) dy}{\int_0^{y_1(t)} f(y) dy}.$$

Note the second term is what we found for the case of a single fixed velocity, if we set $w_0 = \bar{w}$ in Section 4.8. Since $y_1 \leq \frac{u_1-u_0}{\alpha} = t_c^*$, we've shown previously that this term is much less than unity if $t_c^* < 1$. If $y_1 \leq 1$, then the ratio of integrals in the third term is also less than unity, and this term can only be larger than unity if $\alpha \gg h$. The parameter values used in Section 5.1, which were chosen to be typical for these

types of experiments, yield $\frac{\alpha}{h} \approx 0.0435$ and $\frac{w_0}{h} \approx 0.0178$. Thus when $y_1(t) \leq 1$, we see the error in the inferred areal mass cannot exceed approximately 6%. The excellent agreement between the true and inferred areal masses computed in Section 5.1 is consistent with this analysis.

5.3 General case: Arbitrary time dependence, single arbitrary velocity

Now consider the case where the areal mass function at the source has an arbitrary time dependence and a single time-dependent velocity with its own arbitrary time dependence. This can be expressed

$$m_c(w, t_c) = f(t_c) \delta[w - \varphi(t_c)]. \quad (5.12)$$

where $\varphi(t_c)$ is an invertible function with units of velocity.

If we denote $g(t_c) = w - \varphi(t_c)$, then $g'(t_c) = -\varphi'(t_c)$ and $g(\hat{t}_c) = 0 \implies \hat{t}_c(w) = \varphi^{-1}(w)$. Then

$$m_c(w, t_c) = \frac{f(t_c)}{\left| -\varphi'[\varphi^{-1}(w)] \right|} \delta[t_c - \hat{t}_c(w)]$$

and

$$m_a(u, t) = \left(\frac{u}{u - u_{fs}} \right) \frac{1}{\left| -\varphi'[\varphi^{-1}(u - u_{fs})] \right|} f\left(\frac{ut - h}{u - u_{fs}}\right) \delta\left[\frac{ut - h}{u - u_{fs}} - \varphi^{-1}(u - u_{fs})\right].$$

Let

$$j(t) \equiv \frac{ut - h}{u - u_{fs}} - \varphi^{-1}(u - u_{fs}).$$

Then

$$|j'(t)| = \frac{u}{u - u_{fs}}$$

and

$$j(\hat{t}) = 0 \implies \hat{t}(u) = \frac{h}{u} + \frac{(u - u_{fs}) \varphi^{-1}(u - u_{fs})}{u},$$

so

$$\delta[j(t)] = \left(\frac{u - u_{fs}}{u} \right) \delta[t - \hat{t}(u)]$$

and we can write

$$m_a(u, t) = \frac{1}{\left| -\varphi'[\varphi^{-1}(u - u_{fs})] \right|} f\left(\frac{ut - h}{u - u_{fs}}\right) \delta[t - \hat{t}(u)].$$

The true accumulated areal mass at the sensor is

$$m_t(t) = \int_0^t \int_0^\infty m_a(u, t') du dt' = \int_0^t \int_0^\infty \frac{1}{\left| -\varphi'[\varphi^{-1}(u - u_{fs})] \right|} f\left(\frac{ut' - h}{u - u_{fs}}\right) \delta[t' - \hat{t}(u)] du dt'.$$

It's preferable to flip the order of integrations so that we can use the sifting property of $\delta[t']$. The delta function will have a nonzero contribution as long as $0 < \hat{t}(u) < t$ for a fixed velocity u , or

$$\varphi^{-1}(u - u_{fs}) < \frac{ut - h}{u - u_{fs}} = t_c(w, t).$$

This condition sets an upper limit on the velocity integration, which we will denote $\bar{u}(t)$. Then

$$\begin{aligned} m_t(t) &= \int_{u_0}^{\bar{u}(t)} du \int_0^t \frac{1}{\left| -\varphi'[\varphi^{-1}(u - u_{fs})] \right|} f\left(\frac{ut' - h}{u - u_{fs}}\right) \delta[t' - \hat{t}(u)] dt' \\ &= \int_{u_0}^{\bar{u}(t)} \frac{1}{\left| -\varphi'[\varphi^{-1}(u - u_{fs})] \right|} f\left[\frac{u\hat{t}(u) - h}{u - u_{fs}}\right] du. \end{aligned}$$

Since

$$\frac{u\hat{t}(u) - h}{u - u_{fs}} = \frac{1}{u - u_{fs}} \left\{ u \left[\frac{h}{u} + \left(\frac{u - u_{fs}}{u} \right) \varphi^{-1}(u - u_{fs}) \right] - h \right\} = \varphi^{-1}(u - u_{fs})$$

the true accumulated areal mass at the sensor is

$$m_t(t) = \int_{u_0}^{\bar{u}(t)} \frac{f[\varphi^{-1}(u - u_{fs})]}{\left| -\varphi'[\varphi^{-1}(u - u_{fs})] \right|} du.$$

Similarly, the inferred accumulated areal mass at the sensor is

$$m_i(t) = \frac{1}{h} \int_0^t \int_0^\infty m_a(u, t') u t' du dt'$$

$$\begin{aligned}
&= \frac{1}{h} \int_{u_0}^{\bar{u}(t)} du \int_0^t \frac{1}{\left| -\varphi'[\varphi^{-1}(u - u_{fs})] \right|} f\left(\frac{ut' - h}{u - u_{fs}}\right) \delta[t' - \hat{t}(u)] u t' dt' \\
&= \frac{1}{h} \int_{u_0}^{\bar{u}(t)} \frac{f[\varphi^{-1}(u - u_{fs})]}{\left| -\varphi'[\varphi^{-1}(u - u_{fs})] \right|} u \hat{t}(u) du \\
&= \frac{1}{h} \int_{u_0}^{\bar{u}(t)} \frac{f[\varphi^{-1}(u - u_{fs})]}{\left| -\varphi'[\varphi^{-1}(u - u_{fs})] \right|} [h + (u - u_{fs})\varphi^{-1}(u - u_{fs})] du \\
&= \int_{u_0}^{\bar{u}(t)} \frac{f[\varphi^{-1}(u - u_{fs})]}{\left| -\varphi'[\varphi^{-1}(u - u_{fs})] \right|} du + \frac{1}{h} \int_{u_0}^{\bar{u}(t)} \frac{(u - u_{fs})\varphi^{-1}(u - u_{fs})f[\varphi^{-1}(u - u_{fs})]}{\left| -\varphi'[\varphi^{-1}(u - u_{fs})] \right|} du \\
&= m_t(t) + \frac{1}{h} \int_{u_0}^{\bar{u}(t)} \frac{(u - u_{fs})\varphi^{-1}(u - u_{fs})f[\varphi^{-1}(u - u_{fs})]}{\left| -\varphi'[\varphi^{-1}(u - u_{fs})] \right|} du.
\end{aligned}$$

If we make the natural substitution $w = u - u_{fs}$, then define $\bar{w}(t) \equiv \bar{u}(t) - u_{fs}$ and $w_0 = u_0 - u_{fs}$, we obtain

$$m_t(t) = \int_{w_0}^{\bar{w}(t)} \frac{f[\varphi^{-1}(w)]}{\left| -\varphi'[\varphi^{-1}(w)] \right|} dw$$

and

$$m_i(t) = m_t(t) + \frac{1}{h} \int_{w_0}^{\bar{w}(t)} w \varphi^{-1}(w) \frac{f[\varphi^{-1}(w)]}{\left| -\varphi'[\varphi^{-1}(w)] \right|} dw.$$

As a test, let $\varphi(t_c) = w_0 + \alpha t_c$. Then $\varphi^{-1}(w) = \frac{w - w_0}{\alpha}$ and $\varphi'(t_c) = \alpha$, so

$$\frac{m_i(t)}{m_t(t)} = 1 + \frac{1}{h} \cdot \frac{\int_{w_0}^{\bar{w}(t)} w \left(\frac{w - w_0}{\alpha}\right) \frac{1}{\alpha} f\left(\frac{w - w_0}{\alpha}\right) dw}{\int_{w_0}^{\bar{w}(t)} \frac{1}{\alpha} f\left(\frac{w - w_0}{\alpha}\right) dw}.$$

Now let $y \equiv \frac{w - w_0}{\alpha}$, and $\bar{y}(t) \equiv \frac{\bar{w}(t) - w_0}{\alpha}$. Then

$$\chi(t) = 1 + \frac{1}{h} \cdot \frac{\int_0^{\bar{y}} (\alpha y + w_0) y f(y) dy}{\int_0^{\bar{y}(t)} f(y) dy} = 1 + \frac{w_0}{h} \cdot \frac{\int_0^{\bar{y}(t)} y f(y) dy}{\int_0^{\bar{y}(t)} f(y) dy} + \frac{\alpha}{h} \cdot \frac{\int_0^{\bar{y}(t)} y^2 f(y) dy}{\int_0^{\bar{y}(t)} f(y) dy}.$$

This is consistent with the result obtained in Section 5.2.

A Inference of Dynamical Quantities and Ejecta Areal Mass from Piezoelectric Voltages

The following discussion follows Appendix B of [7]. In what follows, we make these assumptions:

1. There are no mass sources or sinks in the ejecta cloud (i.e., $dm/dt = 0$).
2. All ejecta motion is collinear, and the ejecta particles have a long mean free path to scattering with each other.
3. Ejecta particles come to rest instantaneously at the pin.
4. Each particle deposits 100% of its momentum upon the pin (i.e., every particle collides perfectly inelastically with the sensor).

Consider a cloud of ejecta particles with mass m and velocity u . Figure 14 depicts a simple cartoon for the momentum deposition on a circular pin head of area A during a time interval Δt .

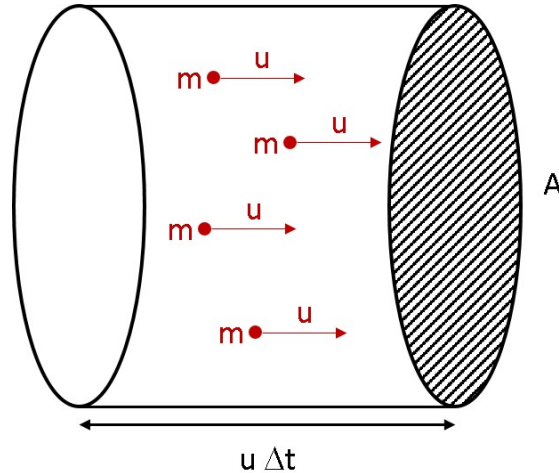


Figure 14: Cartoon model for momentum deposition at the pin head.

The total momentum deposited upon area A in time Δt is $\Delta p = Mu$, where M is the total mass of the cylindrical ejecta cloud. If we let ρ^* denote the mean density of the entire cloud (i.e., the average of many small ejecta particles of mass m within a larger volume of vacuum), then $M = \rho^*V = \rho^*Au\Delta t$, and thus $\Delta p = \rho^*Au^2\Delta t$. The total impulse delivered to the pin over this interval is $F\Delta t = \Delta p$, and therefore the delivered force if $F = A\rho^*u^2$. The instantaneous pressure on the pin in this cartoon model is therefore $P(t) = \rho^*(t)u^2(t)$. This is equivalent to the dynamical ram pressure in a hydrodynamic limit where the ejecta cloud is treated as a fluid.

More rigorously, consider the Hamiltonian of the ejecta cloud-piezo pin system, disregarding the restoring forces in the piezoelectric material (which must be present in the physical system, since the crystal must relax between discrete collision events). If

$$H = T + V = \frac{1}{2}mu^2 \quad (\text{A.1})$$

then the force *on the particle* during the collision with the pin is given by

$$\frac{\partial H}{\partial x} = -\frac{dp}{dt} = -F \quad (\text{A.2})$$

and thus the force *on the pin* is given by

$$F = \frac{\partial}{\partial x} \left(\frac{1}{2}mu^2 \right), \quad (\text{A.3})$$

which, from above, leads to the relationship

$$m \frac{\partial u}{\partial x} = A\rho^*u. \quad (\text{A.4})$$

The piezoelectric sensor is a pressure transducer; it registers a change in the applied pressure. (As pointed out in [7], the sensor must create a voltage when the applied force *changes*, as otherwise the sensor could be used to generate arbitrary amounts of charge, thereby violating the conservation of energy.) If V is the voltage produced by the sensor over a terminating resistance R [Ω], and if S is the piezoelectric sensitivity [C/N], then the relationship is given by

$$\frac{dP}{dt} = \frac{V(t)}{ARS} \quad (\text{A.5})$$

or

$$P(t) = \frac{1}{ARS} \int_0^t V(t') dt' \approx \rho^*(t)u^2(t). \quad (\text{A.6})$$

Thus the pressure (or force) on the pin head is the most fundamental dynamical quantity obtained from the sensor voltage trace. Under the appropriate assumptions, this pressure is equivalent to the dynamical ram pressure of the ejecta cloud impinging upon the sensor.

We now make the following additional assumptions:

5. All ejecta are produced instantaneously at the moment of surface release (i.e., when the shock breaks out from the free surface).
6. Surface motion is negligible during the instant of release.
7. The velocity of each ejecta particle is constant between the free surface and the sensor.

Under these conditions, an ejecta particle arriving at the sensor at time t must have velocity $v(t) = h/(t - t_0)$ where t_0 is the breakout time and h is the distance between the free surface and the sensor. In other words, under assumptions 5-7 the velocity is determined from the time of flight. When this holds, we can obtain the mean density of the ejecta cloud directly from the pressure:

$$\rho^*(t) = \frac{P(t)}{v^2(t)}. \quad (\text{A.7})$$

From Figure 14, it is clear the mass deposition Δm over a time interval Δt in this cartoon model is given by $\Delta m = \rho^* V = \rho^* A v \Delta t$, and thus in the infinitesimal limit the ejecta areal mass inferred from the sensor voltage trace is

$$m_i(t) = \frac{dm}{dA}(t) = \int_0^t \rho^*(t') v(t') dt' = \int_0^t \frac{P(t')}{v(t')} dt' = \int_0^t \left(\frac{t' - t_0}{h} \right) P(t') dt' \quad (\text{A.8})$$

where $P(t)$ is given by Equation A.6.

References

- [1] Vogan, W. S., Anderson, W. W., Grover, M., Hammerberg, J. E., King, N. S. P., Lamoreaux, S. K., Macrum, G., Morley, K. B., Rigg, P. A., Stevens, G. D., Turley, W. D., Veeser, L. R., Buttler, W. T. “Piezoelectric characterization of ejecta from shocked tin surfaces,” *J. Appl. Phys.* **98** 113508 (2005).
- [2] Zellner, M. B., Grover, M., Hammerberg, J. E., Hixson, R. S., Iverson, A. J., Macrum, G. S., Morley, K. B., Obst, A. W., Olson, R. T., Payton, J. R., Rigg, P. A., Routley, N., Stevens, G. D., Turley, W. D., Veeser, L., Buttler, W. T. “Effects of shock-breakout pressure on ejection of micron-scale material from shocked tin surfaces,” *J. Appl. Phys.* **102** 013522 (2007).
- [3] Monfared, S. K., Oró, D. M., Grover, M., Hammerberg, J. E., LaLone, B. M., Pack, C. L., Schauer, M. M., Stevens, G. D., Stone, J. B., Turley, W. D., Buttler, W. T. “Experimental observations on the links between surface perturbation parameters and shock-induced mass ejection,” *J. Appl. Phys.* **116** 063504 (2014).
- [4] Buttler, W. T., Oró, D. M., Preston, D. L., Mikaelian, K. O., Cherne, F. J., Hixson, R. S., Mariam, F. G., Morris, C., Stone, J. B., Terrones, G., Tupa, D. “Unstable Richtmyer-Meshkov growth of solid and liquid metals in vacuum,” *J. Fluid Mech.* **703** 60 (2012).
- [5] Dimonte, Guy, Terrones, Guillermo, Cherne, F. J., Ramaprabhu, P. “Ejecta source model based on the nonlinear Richtmyer-Meshkov instability,” *J. Appl. Phys.* **113** 024905 (2013).
- [6] Cherne, F. J., Hammerberg, J. E., Andrews, M. J., Karkhanis, V., Ramaprabhu, P. “On Shock Driven Jetting of Liquid from Non-Sinusoidal Surfaces into a Vacuum,” *J. Appl. Phys.* **118** 185901 (2015).
- [7] Buttler, W. T., Oró, D. M., Olson, R. T., Cherne, F. J., Hammerberg, J. E., Hixson, R. S., Monfared, S. K., Pack, C. L., Rigg, P. A., Stone, J. B., Terrones, G. “Second shock ejecta measurements with an explosively driven two-shockwave drive,” *J. Appl. Phys.* **116** 103519 (2014).